ELSEVIER

Biochimica et Biophysica Acta 1366 (1998) 331–354

BIOCHIMICA ET BIOPHYSICA ACTA

BBA

Correction[1]

Infrared spectroscopic identification of the C–O stretching vibration associated with the tyrosyl Z• and D• radicals in photosystem II[2]

Sunyoung Kim, Idelisa Ayala, Jacqueline J. Steenhuis, Enid T. Gonzalez, M. Reza Razeghifard, Bridgette A. Barry *

University of Minnesota, College of Biological Sciences, Department of Biochemistry, St. Paul, MN 55108, USA

Received 27 January 1998; accepted 7 July 1998

Abstract

Photosystem II (PSII) is a multisubunit complex, which catalyzes the photo-induced oxidation of water and reduction of plastoquinone. Difference Fourier-transform infrared (FT-IR) spectroscopy can be used to obtain information about the structural changes accompanying oxidation of the redox-active tyrosines, D and Z, in PSII. The focus of our work is the assignment of the 1478 cm^{-1} vibration, which is observable in difference infrared spectra associated with these tyrosyl radicals. The first set of FT-IR experiments is performed with continuous illumination. Use of cyanobacterial strains, in which isotopomers of tyrosine have been incorporated, supports the assignment of a positive 1478/1477 cm^{-1} mode to the C–O stretching vibration of the tyrosyl radicals. In negative controls, the intensity of this spectral feature decreases. The negative controls involve the use of inhibitors or site-directed mutants, in which the oxidation of Z or D is eliminated, respectively. The assignment of the 1478/1477 cm^{-1} vibrational mode is also based on control EPR and fluorescence measurements, which demonstrate that no detectable $Fe^{2+}Q_A^-$ signal is generated under FT-IR experimental conditions. Additionally, the difference infrared spectrum, associated with formation of the $S_2Q_A^-$ state, argues against the assignment of the positive 1478 cm^{-1} line to the C–O vibration of Q_A^-. In the second set of FT-IR experiments, single turnover flashes are employed, and infrared difference spectra are recorded as a function of time after photoexcitation. Comparison to kinetic transients generated in control EPR experiments shows that the decay of the 1477 cm^{-1} line precisely parallels the decay of the D• EPR signal. Taken together, these two experimental approaches strongly support the assignment of a component of the 1478/1477 cm^{-1} vibrational lines to the C–O stretching modes of tyrosyl radicals in PSII. Possible reasons for the

Abbreviations: chl, chlorophyll; D, tyrosine 160 in the D2 polypeptide of *Synechocystis* 6803 PSII; DCBQ, 2,6-dichloro-*p*-benzoquinone; ENDOR, electron nuclear double resonance; DCMU, 3-(3,4-dichlorophenyl)-1,1-dimethylurea; EPR, electron paramagnetic resonance spectroscopy; ESEEM, electron spin echo envelope modulation; FT-IR, Fourier-transform infrared spectroscopy; HEPES, *N*-(2-hydroxyethyl)piperazine-*N*′-(2-ethanesulfonic acid); MES, 2-(*N*-morpholino)ethanesulfonic acid; PSII, photosystem II; OGP, octyl-β-glucopyranoside; PMS, phenazine methosulfate; TES, *N*-tris(hydroxymethyl)methyl-2-aminoethanesulfonic acid; Tris, tris(hydroxylmethyl)aminomethane; Z, tyrosine 161 in the D1 polypeptide of *Synechocystis* 6803 PSII

* Corresponding author. University of Minnesota, Dept. of Biochemistry, 1479 Gortner Avenue, St. Paul, MN 55108, USA. Fax: +1-612-625-5780; E-mail: barry@biosci.cbs.umn.edu

[1] This paper is reprinted in its entirety from Volume 1364 (1998) 337–360, as several errors went uncorrected by the publisher, who apologises to authors and readers for this unfortunate mishap.

[2] Supported by NIH GM 43272 (B.A.B.), NSF MCB 94-18164 (B.A.B.), a graduate minority supplement to NIH GM 43273 (I.A.), a graduate fellowship from Committee on Institutional Cooperation, University of Minnesota (I.A.), and a summer research fellowship from Dupont, Central Research and Development, administered through the University of Minnesota (E.T.G.).

PII: S0005-2728(98)00133-9

apparently contradictory results of Hienerwadel et al. (Biochemistry 35 (1996) 15447–15460 and Biochemistry 36 (1997) 14705–14711) are discussed.

Keywords: Photosystem II; Tyrosine Z; Q_A; FT-IR; EPR; Fluorescence; Isotopic labeling; Tyrosine D

1. Introduction

Photosystem II (PSII), which is a multisubunit complex of both hydrophobic and hydrophilic subunits, is responsible for the oxidation of water and production of reduced plastoquinone. Several cofactors and amino acids, located in the hydrophobic subunits of PSII, are obligatory for charge separation and oxygen production. Four consecutive charge separations in the PSII reaction center create the oxidizing equivalents necessary for the oxidation of two molecules of water to molecular oxygen. This process occurs at a tetranuclear manganese cluster (reviewed in Refs. [1,2]).

Two polypeptides, termed D1 (32 kDa) and D2 (34 kDa), form the heterodimer core of the PSII reaction center [3] and bind the majority of cofactors involved in electron transfer, such as the primary chlorophyll donor (P_{680}), pheophytin, quinones, and nonheme iron. After photoexcitation, P_{680} rapidly transfers an electron to a pheophytin molecule (for example, see Refs. [4–7] and references therein). Pheophytin, in turn, reduces a bound quinone, Q_A [8–11]. Reduced Q_A transfers an electron to the two electron gate, Q_B, in microseconds [12]. To guarantee efficiency and decrease probability of back reactions, P^+_{680} must be reduced before the electron is transferred to Q_B. P^+_{680} is reduced by a tyrosine, which in turn forms a radical Z• within nanoseconds [13]. The tyrosine radical is then reduced by the manganese cluster in micro- to millisecond time scale, dependent upon the Mn cluster oxidation state [14–16].

Reduction of tyrosine Z• can be slowed by removal of the manganese cluster [17]. Removal of the manganese cluster permits photoaccumulation of an EPR signal from Z• [18,19]. Z• has been identified as a tyrosine radical through EPR and isotopic labeling of PSII particles isolated from cyanobacteria [20]. Site-directed mutagenesis experiments demonstrate that Z is Y161 of D1 [21–23]. Tyrosine Z is required for oxygen evolution [21–23]. The presence of a disordered hydrogen bond to the tyrosyl Z• radical in site-directed mutants has been suggested by magnetic resonance and high-field EPR investigations [24–26], but see Ref. [27].

A second redox-active tyrosine associated with PSII is the dark stable radical D•. This species was identified as a tyrosine radical through the use of isotopic labeling and EPR spectroscopy [28]. Site-directed mutagenesis defined D as residue 160 in the D2 polypeptide [29,30]. The function of the tyrosine D is unknown, but tyrosine D is oxidized via P^+_{680} and the manganese cluster [31,32]. In the absence of the manganese cluster, tyrosine D is oxidized directly by P^+_{680} [33]. Replacement of tyrosine D with either phenylalanine (YF160D2) or tryptophan did not eradicate activity, indicating that tyrosine D is not required for oxygen evolution [29,30,34]. A hydrogen bond to the phenolic oxygen of tyrosyl D• radical has been observed by ESEEM [35], ENDOR [36,37], high-field EPR [25], and infrared spectroscopies [27].

In contrast to the magnetic resonance spectroscopies that selectively probe the paramagnetic species, infrared spectroscopy can delineate the interactions of Z• and D• with the surrounding protein environment. Fourier-transform infrared (FT-IR) spectroscopy is a vibrational technique that monitors changes in the dipole moment of chemical bonds. FT-IR spectroscopy is still a relatively new technique in its application to PSII. In the absence of molecular symmetry constraints, each of these vibrations is potentially observable in infrared spectroscopy as an absorption or vibrational line. When vibrational spectroscopy is applied to the examination of a protein, vibrations may be classified into three categories: (1) vibrations of the peptide bond, which are often delocalized on the peptide backbone; (2) vibrations associated with amino acid side chains; and (3) vibrations associated with prosthetic and chromophore groups. Infrared spectroscopy is sensitive to the interaction of a chemical moiety with its protein environment, as well as to its geometry and protonation state.

Structural changes that accompany function can be examined selectively using difference FT-IR spectroscopy. Difference FT-IR spectroscopy identifies vibrations associated with amino acid side chains or prosthetic groups, which are perturbed upon the transition between two functional states of the protein. Light-minus-dark difference spectra measure the structural alterations associated with light-induced biological processes. The sensitivity of this spectroscopic technique is sufficient to detect vibrational modes from single amino acid residues, even against a large absorption background. The usefulness of this technique, in application to membrane proteins, was first demonstrated in studies of bacteriorhodopsin (for example, see Refs. [38–40]).

The major restriction of this difference infrared technique is the required, intricate analyses of the spectra generated (for review, see Ref. [41]). Furthermore, assignment of IR signals can be confused by heterogeneous, overlapping bands. As reviewed [1], this difficulty in analysis is evident in the disagreements in the literature regarding the assignment of a line at 1478 cm^{-1} in the vibrational difference spectra of PSII. This line has been assigned both to acceptor side radicals [42–46] and to donor side species [27,47–51].

Here, we describe experiments aimed at the assignment of the 1478 cm^{-1} line. We first describe our methodology for obtaining difference FT-IR spectra, using continuous illumination, at pH 7.5. This method allows us to obtain the vibrational spectra associated with the oxidation of tyrosine Z and of tyrosine D in PSII, independent of contributions from the acceptor side. We compare these data, which have no detectable contribution from Q_A^-, to spectra obtained under conditions in which the acceptor side is expected to contribute to the spectrum. This comparison supports the assignment of vibrational modes, observed at pH 7.5, at 1478 and 1477 cm^{-1} to D• and Z• and not to Q_A^-. This conclusion is validated by kinetic infrared transients, obtained using flash illumination. These experiments show that the decay of the 1477 cm^{-1} line superimposes on the decay of the EPR signal of tyrosyl radical, D•. To our knowledge, this is the first study to use superposition of kinetic transients to assign vibrational features in PSII. Finally, examination of PSII samples in which tyrosine, but not plastoquinone or chlorophyll, is isotopically labeled, and negative controls, in which the tyrosines are not oxidized, allows assignment of the 1478/1477 cm^{-1} lines to normal modes involving the C–O stretching vibrations of tyrosyl Z• and D• radicals.

2. Materials and methods

2.1. Spinach PSII purification and manganese depletion

PSII membranes, containing 274 chl per reaction center [52], were isolated from market spinach [53]. The membranes were resuspended in a buffer containing 0.4 M sucrose, 50 mM MES-NaOH, pH 6.0 and 15 mM NaCl. From the above PSII preparations, an OGP-solubilized PSII core preparation [54], containing the extrinsic manganese-stabilizing subunit (33 kDa) and 78 chl per reaction center [52], was obtained.

For manganese depletion, PSII membranes or PSII core preparations were incubated in an equal volume of a buffer containing 1.6 M Tris-HCl, pH 8.0, and 4 mM EDTA for 20 min in light at 4°C. For PSII core preparations, after centrifugation for 30 min at $40\,000 \times g$, the pellet was resuspended in five volumes of 5 mM HEPES-NaOH, pH 7.5 and centrifuged for 30 min at $40\,000 \times g$. The final pellet was resuspended in 5 mM HEPES-NaOH, pH 7.5 and 0.03% lauryl maltoside (Anatrace, OH) to a final concentration of 1–15 mg chl ml^{-1}. For PSII membranes, immediately following Tris treatment, samples were incubated and washed in successive rounds of N_2-degassed 50 mM phosphate, pH 6.0, 100 mM formate, 10 mM NaCl, 15 mM $MgCl_2$ and of 50 mM phosphate, pH 6.0, 50 mM formate, 10 mM NaCl, 15 mM $MgCl_2$, as described in [44]; the final pellet was resuspended in 50 mM phosphate, pH 6.0, 50 mM formate, 10 mM NaCl, 15 mM $MgCl_2$ to a concentration of 3.7 mg chl ml^{-1}. Tris-washed PSII membranes were also resuspended in 5 mM HEPES-NaOH, pH 7.5, as described for the PSII core preparations, with the identical number of wash steps employed for the phosphate/formate treatment; the final pellet was resuspended in 5 mM HEPES-NaOH, pH 7.5, to a concentration of 3.4 mg chl ml^{-1}. Both Tris-washed PSII membranes in phosphate/formate, pH 6.0, and

in 5 mM HEPES-NaOH, pH 7.5, were used immediately for spectroscopy.

2.2. Growth of Synechocystis sp. PCC 6803 and cyanobacterial PSII protein purification

Glucose-tolerant wildtype strains were photoheterotrophically grown, as described [55], in BG-11 medium [56] supplemented with 5 mM TES-NaOH, pH 8.0, and sterile-filtered 5 mM glucose under constant illumination at 30°C. Cells from 15-liter carboys were harvested by centrifugation after 7 days, when culture reached approximately 1.0 $OD_{730\,nm}$.

PSII particles were purified from the above wildtype cyanobacterial cultures [57,58] or from cultures of the YF160D2 mutant, which lacks tyrosine D [29,34]. A thylakoid membrane preparation was obtained from the harvested cells. A two-step chromatographic purification of PSII from the lauryl maltoside-solubilized thylakoid prep was employed: (1) a 90 ml Fast Flow Q-Sepharose (Pharmacia) gel column at pH 6.0, for an initial partial purification of PSII, and (2) a Pharmacia HR 5/5 MonoQ FPLC column. Several MonoQ columns, with approximately 1 mg chl loaded per column, were run from a single Fast Flow Q column. For each *Synechocystis* strain, material from several carboys was pooled together at the MonoQ purification.

2.3. Manganese depletion of cyanobacterial PSII

For some experiments, manganese was depleted from *Synechocystis* PSII samples by methods previously described [27,47]. Protein samples were incubated in the presence of 10 mM NH_2OH at 0°C for 40 min in darkness with gentle mixing [59]. A 50 mM NH_2OH stock solution was made in low-salt buffer, and the pH was adjusted to 6.0 with NaOH, shortly before use. After hydroxylamine treatment, the sample was diluted 1:1 (v/v) with low-salt buffer. NH_2OH-treated PSII particles were concentrated by binding the preparation to a MonoQ 5/5 HR column [60]. The protein sample remains bound to the top of the MonoQ column. The column was washed with 15 ml low-salt buffer. The column was inverted, and the sample was eluted with 275 mM NaCl; this elution performed on the inverted column prevents dilution of the sample through the column bed and permits the protein sample to be collected in a concentrated form. The concentrated sample was dialyzed overnight against 5 mM HEPES-NaOH pH 7.5. All dialyzed samples were concentrated in Centricon 100 concentrators (Amicon, Beverly, MA) to approximately 1 mg chl ml^{-1}, aliquoted, frozen in liquid nitrogen, and stored at −80°C until use.

2.4. Chlorophyll and oxygen evolution assays

Chlorophyll determination in spinach and in cyanobacterial preparations was in 80% acetone or 100% methanol, respectively [61]. Steady-state rates of oxygen evolution were measured in a water-jacketed cuvette (1.5 ml) at 25°C with 10–20 μg chl. Saturating actinic light was provided by a red-filtered fiber-optic light source (Dolan Jenner). Assay buffer for spinach PSII preparations contained 0.4 M sucrose, 50 mM MES-NaOH, pH 6.0, and 10 mM $CaCl_2$, whereas the assay buffer for cyanobacterial PSII preparations contained 1 M sucrose, 50 mM MES-NaOH, pH 6.5, 25 mM $CaCl_2$, and 10 mM NaCl. Exogenous acceptors were 1 mM re-crystallized 2,6-DCBQ and 1 mM potassium ferricyanide. Air-saturated water was used as an oxygen standard. The initial rate of activity was derived from the average rate of oxygen evolution between 12 and 30 s after the beginning of illumination. Oxygen rates of isolated PSII preparations before manganese depletion were as follows: (a) spinach membranes, 1000; (b) spinach, OGP-derived, preparation, 1800; (c) wildtype (cyanobacterial), 2700; (d) $^{13}C(6)$-labeled wildtype, 2400; (e) $^{13}C(1)$-labeled wildtype, 2300; (f) 3,5-$^{2}H(2)$-labeled wildtype, 2400; and (g) YF160D2, 700 μmol O_2 mg^{-1} chl h^{-1}.

2.5. Isotopic labeling of tyrosines in cyanobacterial wildtype cultures

The redox-active tyrosines in PSII can be isotopically labeled by supplying *Synechocystis* 6803 labeled tyrosine under conditions where the organism is a functional auxotroph for the amino acid [28]. Cultures of *Synechocystis* were grown on 5 mM kanamycin sulfate, 0.5 mM phenylalanine, 0.25 mM tryptophan, and 0.25 mM of one of the following: control tyrosine, $^{13}C(6)$-tyrosine {(L-4-hydroxyphen-

yl-$^{13}C_6$)-alanine}, $^{13}C(1)$-tyrosine {(L-4-hydroxyphenyl-$^{13}C_1$)-alanine}, or 3,5-$^{2}H(2)$-tyrosine {(L-4-hydroxyphenyl-3,5-$^{2}H_2$)-alanine} (99% labeled, Isotec, Miamisburg, OH) [28]; amino acids were added by sterile filtration. Cells were harvested, when the $OD_{730\,nm}$ was approximately 0.6–0.7. Cells grown under these conditions required modifications to the PSII purification protocol [58]. Samples were purified [20] and depleted of manganese, as described above, in one day.

2.6. EPR spectroscopy

A Bruker EMX 6/1 EPR spectrometer equipped with a Bruker ST-TE cavity and a Wilmad variable temperature dewar was employed. A stream of cold nitrogen was used to maintain the EPR sample at the desired temperature. Continuous illumination in the cavity was provided with a red-filtered (Dolan Jenner FRI-50 filter) light from a fiber-optic illuminator (Dolan Jenner, Woburn, MA).

For control experiments on tyrosyl radicals in cyanobacterial PSII, a manganese-depleted wildtype, cyanobacterial sample at pH 7.5 (80 μg @ 1.0 mg chl ml^{-1}) was dried on mylar strips [47] with 3 mM ferricyanide and 3 mM ferrocyanide. Spectral conditions were: microwave frequency, 9.4 GHz; power, 0.5 mW; modulation amplitude, 3.5 G; scan time, 252 s; time constant, 1.3 s; and temperature, −9°C. Spin quantitations were performed under nonsaturating conditions at 200 K, using Fremy's salt, $K_2(SO_3)_2NO$, as a spin standard [62]. Samples were illuminated in the EPR cavity.

For control experiments comparing the yield of tyrosyl radicals in spinach, Tris-washed membranes in phosphate/formate or HEPES, 300 μl of aqueous samples were employed. For the Tris-washed PSII membranes in 5 mM HEPES, pH 7.5, 50 mM stocks of potassium ferricyanide and potassium ferrocyanide were diluted into the sample to obtain a final concentration of 3 mM ferricyanide and 3 mM ferrocyanide. For the Tris-washed PSII membranes in phosphate/formate, pH 6.0, a 400 mM stock of potassium ferricyanide was diluted into the sample to obtain a final concentration of 2150 mol ferricyanide per mol reaction center, or 64 mM ferricyanide, as employed previously [44,45]. For both samples spectral conditions were: microwave frequency, 9.4 GHz; power, 0.5 mW; modulation amplitude, 3.2 G; scan time, 41.9 s; time constant, 1.3 s; gain, 0.5×10^6. Samples were illuminated in the EPR cavity.

For kinetic experiments on spinach OGP-derived PSII preparations, the second harmonic of a Continuum (Santa Clara, CA) Nd-YAG laser was employed as the illumination source. The laser was externally triggered using a NB-TIO-10 board (National Instruments, Austin, TX) and a Macintosh computer. The pulse width was <7 ns, and the power density on the sample was 10 mJ cm^{-2}. Samples were flashed in the EPR cavity.

Spinach, manganese-depleted OGP samples, containing 80 or 160 μg of the spinach core preparation, 3 mM potassium ferricyanide, and 3 mM potassium ferrocyanide, were dried on mylar strips [47]. To measure Z• decay, 50 laser flashes were used. The time between the flashes was 5 s. Spectral conditions were: microwave frequency: 9.4 GHz; field setting, 3338 G; power, 13 mW; modulation amplitude, 5 G; scan time, 1.3 s; time constant, 10.2 ms.

To measure D• decay on spinach, manganese-depleted OGP samples, either 8 consecutive flashes were fired into the EPR cavity, and a 10 min scan was acquired, or 1 flash was fired at 132 s intervals into the EPR cavity. Spectral conditions were: microwave frequency: 9.4 GHz; field setting, 3338 G; power, 13 mW; modulation amplitude, 4 G; time constant, 20.5 ms.

In some experiments on spinach, manganese-depleted OGP samples, continuous illumination in the cavity was employed. Spectral conditions were: microwave frequency, 9.4 GHz; power, 0.8 mW; modulation amplitude, 4 G; scan time, 41.9 s; time constant, 1.3 s.

For control experiments evaluating potential acceptor side contributions, $Fe^{2+}Q_A^-$ EPR spectra were recorded at helium temperature on the Bruker X-band spectrometer equipped with an Oxford Instruments cryostat. A 50 mM stock of potassium ferricyanide was diluted into intact cyanobacterial wildtype PSII samples (200 μl @ 1.3 mg chl ml^{-1}) to obtain a ratio of 3 mol ferricyanide per mol PSII reaction center or per 57 mol chl [52]. Manganese-depleted cyanobacterial wildtype PSII samples (200 μl @ 1.3 mg chl ml^{-1}) contained 3 mM potassium ferricyanide and 3 mM potassium ferrocyanide. Continuous illumination at 200 K was performed in a

glass dewar filled with dry ice–ethanol mixture; a 150 W Dolan Jenner (Woburn, MA) illuminator with red and heat filters was the light source. Immediately after illumination, samples were flash frozen, by direct submersion in liquid nitrogen, in less than 2 s, and stored in liquid nitrogen, until placed in EPR cavity for measurement. Spectra were recorded at 4.3 ± 0.2 K. Control EPR spectra were obtained first in the tyrosyl spectral region at $g = 2.0$; spectral conditions for tyrosyl spectra at 4 K were: 9.4 GHz; power 0.5 mW; modulation amplitude, 3.2 G; scan time, 336 s; and time constant, 328 ms. Spectral conditions for $Fe^{3+}Q_A$ or $Fe^{2+}Q_A^-$ spectra were: microwave frequency, 9.4 GHz; power, 40 mW; modulation amplitude, 32 G; scan time, 336 s; and time constant, 328 ms.

All EPR spectral manipulations and calculations were performed using the program IGOR Pro (Lake Oswego, OR).

2.7. Difference FT-IR spectroscopy

Infrared data on $S_2Q_A^-$–S_1Q_A in cyanobacterial PSII were obtained by 200 K illumination as described previously [63,64].

Infrared data on tyrosyl radicals in spinach, manganese-depleted OGP samples, obtained using flash illumination, were recorded on a Nicolet (Madison, WI) 60SX spectrometer with a MCT-B detector. Samples, containing 80 μg of the spinach OGP preparation, 3 mM potassium ferricyanide, and 3 mM potassium ferrocyanide, were dried on Ge windows [47]. The germanium window was positioned so as to block illumination of the sample from the He–Ne laser from the optical bench. The sample was then layered with a CaF_2 window. The temperature was maintained at −10°C [47,58]. Spectral resolution was 7.7 cm^{-1}, a Happ–Ganzel apodization function was used, single-sided interferograms, with two levels of zero-filling, were collected, and the mirror velocity was 1.57 cm s^{-1}.

For flash illumination, the Continuum (Santa Clara, CA) laser described above was externally triggered through the use of a NB-TIO-10 board (National Instrument, Austin, TX) and a Macintosh computer. The pulse width was < 7 ns; the power density on the sample was 25 mJ cm^{-2}. Where appropriate, continuous illumination was provided with a red- and heat-filtered fiber-optic equipped Dolan Jenner light source. The light intensity at the sample was 120 μmol s^{-1} m^{-2}.

To acquire spectra in 33 s using flash illumination, 200 mirror scans were collected. Data from 50 flashes were averaged with a time between the flashes of 132 s. EPR control experiments show that this repetition rate is sufficient to allow complete decay of Z• and 64% of D• in the time between flashes. The delay time between laser flash and data acquisition (L1) is estimated to be < 0.7 s. Samples were given a preflash 132 s before data acquisition. Data were ratioed directly to construct the difference spectrum. Difference spectra were then normalized to an amide II absorbance of 0.35.

Infrared data on tyrosyl radicals in wildtype, cyanobacterial PSII, obtained using continuous illumination, were recorded on a Nicolet (Madison, WI) Magna 550 II spectrometer with a MCT-A detector [27,47]. The spectral resolution was 4 cm^{-1}, double-sided interferograms were collected, a Happ–Ganzel apodization function was utilized, and a single level of zero filling was employed. The mirror velocity was 2.5 cm s^{-1}. PSII samples, containing 25–30 μg chlorophyll, 3 mM potassium ferricyanide, and 3 mM potassium ferrocyanide, were pipetted onto a 25 mm (diameter) × 3 mm (thick) germanium window, dried for 25–30 min with a dry nitrogen stream, and then sandwiched with a CaF_2 window. Absorbance at 1655 cm^{-1} (amide I) was always less than 0.4. Temperature was maintained at −9°C by a recirculating water bath, a Harrick constant temperature cell, and Harrick ATC-30D digital temperature controller (Ossining, NY). The sample was illuminated by a Dolan–Jenner illumination system equipped with an A3739 annular fiber-optic light guide, SX-10 adapter, and heat- and red-filters. An Alpha Products (Fairfield, CT) SA-129 R-232 to A-BUS adapter, a ST-143 digital output driver card, and Visual Basic programs were used to interface the OMNIC software with the illumination system. The distance between the light source and the liquid cell in the IR bench was 11 cm; the light intensity at the position of the sample was 75 μmol s^{-1} m^{-2}. The Ge window blocked He–Ne laser illumination of the sample from the FT-IR bench. Four hundred twenty-five scans, taken in 4 min, were coadded for each interferogram. Data recorded in the light were ratioed directly to

data recorded in the dark. Difference spectra were normalized to an amide II absorbance of 0.35. Corrections using the total amount of protein gave similar results, indicating that path length was approximately constant.

2.8. Fluorescence spectroscopy

Spectra were recorded on an Opti-sciences OS-500 modulated fluorometer (Haverhill, MA). Samples were dehydrated onto a glass window and placed in the temperature cell used for FT-IR measurements. Temperature maintenance was performed by the same system described above for FT-IR data acquisition. For fluorescence yield measurements on the cyanobacterial preparation, spectral conditions were: modulation intensity, 180; saturation intensity, 180; time constant, 10 ms; and scan time, 3 s or 4 min. Red-filtered illumination was provided by the fluorometer light source. For fluorescence decay kinetic measurements on the spinach OGP preparation, conditions were: modulation intensity, 180; saturation intensity, 180; time constant, 10 ms; and pulse interval, 20 s or 135 s. Kinetic measurements using 20 and 135 s intervals gave the same result. Transients from 3 sequential pulses were averaged to give the final data shown. Red-filtered illumination was provided by the fluorometer light source; the light was modulated to give 400 ms pulses.

3. Results

3.1. Control EPR experiments for difference FT-IR measurements, employing continuous illumination

In Fig. 1A, we present EPR control experiments, recorded at −9°C, on partially dehydrated, manganese-depleted PSII samples from wildtype *Synechocystis* 6803. These PSII samples, buffered at pH 7.5 to enhance the decay rate of tyrosyl D• [65], contain a mixture of 3 mM potassium ferricyanide and 3 mM potassium ferrocyanide; these PSII samples are identical in biochemical and spectroscopic condition to those employed for infrared measurements. Ferricyanide acts as an exogenous electron acceptor for Q_A^- and ferrocyanide acts as an exogenous electron donor for the donor side of PSII. Q_B is not functional in this preparation (data not shown).

Upon continuous illumination, an EPR spectrum

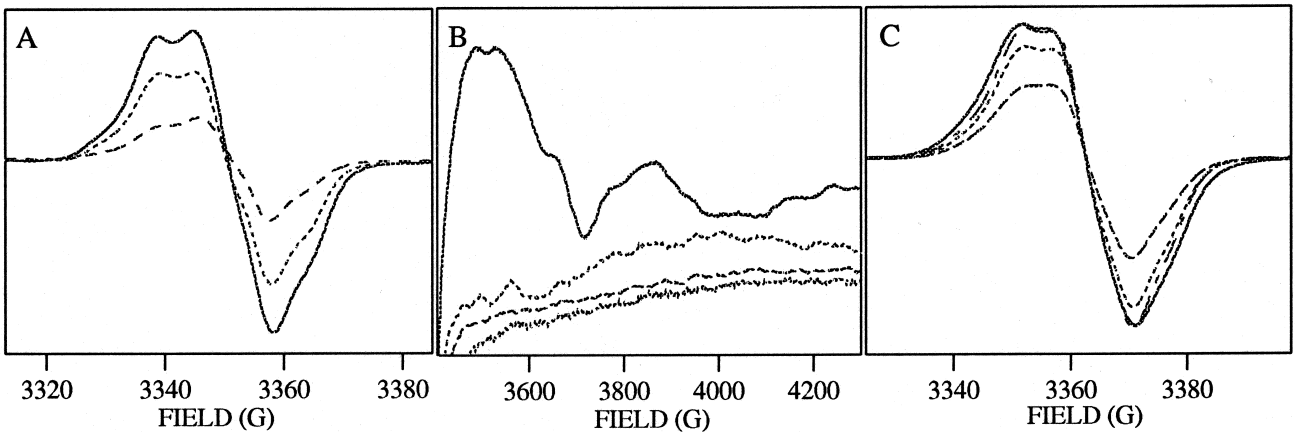

Fig. 1. (A) EPR spectra of tyrosyl radicals in manganese-depleted wildtype *Synechocystis* PSII preparations at pH 7.5. The solid line was recorded under illumination, the dotted line was recorded after a 4 min dark adaptation, and the dashed line was recorded after 32 min dark adaptation. Spectra were acquired at −9°C. (B) EPR spectra of $Fe^{2+}Q_A^-$ in *Synechocystis* PSII preparations at pH 7.5. Oxygen evolving PSII, containing three equivalents of potassium ferricyanide, was dark adapted for 4 min (dotted line); samples were then illuminated at −9°C for 4 min (solid line). Manganese-depleted PSII, containing 3 mM potassium ferricyanide and 3 mM potassium ferrocyanide, was dark adapted for 4 min (hatched line) and illuminated at −9°C for 4 min (dashed line). Samples were illuminated in a dry ice–ethanol bath at −9°C for 4 min, flash-frozen, and stored in liquid nitrogen until EPR measurements were performed. Spectra were acquired at 4 K. (C) EPR spectra of tyrosyl radicals in *Synechocystis* PSII preparations at pH 7.5. Spectra shown are the $g=2$ region of data shown in (B). The PSII sample, containing 3 mM ferri/ferrocyanide, was illuminated at −9°C for 4 min (solid line) and dark adapted for 4 min (dotted line) or illuminated for 4 min (dot–dashed line) and dark adapted for 30 min (dashed line). Spectra were acquired at 4 K.

is acquired (Fig. 1A, solid line), which is a composite spectrum of tyrosyl D• and Z•. As expected, within a 4 min dark adaptation, tyrosyl Z• is reduced, and the resulting EPR spectrum is solely the dark-stable tyrosyl D• radical (Fig. 1A, dotted line). Spin quantitation of this EPR spectrum gives approximately 0.9 spin per reaction center. The D• spectrum shows the expected lineshape with partially resolved hyperfine splittings, a g value of 2.0046, and an approximately 20 G linewidth [66]. This radical is relatively stable, since only 60% of the amplitude is lost in 32 min following continuous illumination (Fig. 1A, dashed line).

EPR spectroscopy was used to examine the yield of semiquinone anion radicals, potentially generated on the acceptor side, in the above PSII samples (Fig. 1B). Photoreduced Q_A is a semiquinone anion radical that interacts with a nearby Fe^{2+} ion; this $Fe^{2+}Q_A^-$ radical generates a $g=1.9$–1.82 and 1.67–1.64 signal in PSII, observable at liquid helium temperatures and with high microwave power {reviewed in Ref. [66]}. The magnitude of the $Fe^{2+}Q_A^-$ EPR signal upon continuous illumination of PSII samples below 230 K is indicative of the fraction of PSII reaction centers that have undergone a stable, single charge separation, as electron transport from Q_A to Q_B is inhibited at these temperatures [67]. As a positive control, we used a PSII sample that contained three equivalents of potassium ferricyanide; these are conditions where the maximum yield of Q_A^- should be trapped by a 4 min illumination and flash freezing, outside the EPR cavity. Upon continuous illumination at −9°C, a $Fe^{2+}Q_A^-$ EPR signal is generated in this cyanobacterial PSII preparation (Fig. 1B, solid line); the amplitude of the signal is equivalent upon continuous illumination at −9°C and 200 K (data not shown). The signal decays in a 4 min dark adaptation (Fig. 1B, dotted line).

However, under the conditions used for infrared spectroscopy, when cyanobacterial PSII samples contain 3 mM ferricyanide and 3 mM ferrocyanide, no detectable $Fe^{2+}Q_A^-$ EPR signal is formed under continuous illumination at −9°C (Fig. 1B, dashed line). The absence of a detectable $Fe^{2+}Q_A^-$ signal upon illumination could result from rapid reoxidation by ferricyanide, before the sample is flash frozen. However, illumination of samples containing 3 mM ferricyanide and 3 mM ferrocyanide traps tyrosyl radical Z• (Fig. 1C, so1id line), arguing that the freezing procedure in liquid nitrogen immediately after illumination is rapid enough for radical trapping. As an additional control for such reoxidation, we will present fluorescence experiments under the same conditions (see below).

Another potential explanation for the lack of a detectable $Fe^{2+}Q_A^-$ EPR signal is the generation of an alternative state of the FeQ_A electron acceptor complex, $Fe^{3+}Q_A$; this state has been generated in some studies in which certain exogenous acceptors were used, high pH values were employed, or PSII subunits were depleted (for example, see Ref. [68]). In this case, the oxidized Fe^{3+} can be reduced by Q_A^-. The turning points of the $Fe^{3+}Q_A$ signal occur at $g=8$ and 5.5, in the absence of DCMU [66]. Examination of the $g=8$ to $g=5$ region of the EPR spectra, shown in Fig. 1B and C, demonstrates that there is no detectable $Fe^{3+}Q_A$ signal in either the positive control or in the PSII sample, containing 3 mM ferricyanide and 3 mM ferrocyanide (data not shown).

This conclusion is supported by examination of these spectra in the $g=2$ region (Fig. 1C). In studies on PSII containing 3 mM ferri/ferrocyanide, illumination traps a tyrosyl radical, Z• (Fig. 1C, solid line), with a normal EPR lineshape. If Fe^{3+} had been produced, reduction of Q_A would be accompanied by generation of a narrow $g=2$ signal from the uncoupled, semiquinone anion radical [69]. Thus, our EPR experiments demonstrate that there is no detectable generation of Q_A^- under the conditions employed for infrared measurements in cyanobacterial PSII.

3.2. Control fluorescence experiments for difference FT-IR measurements, employing continuous illumination

Utilizing a second method to investigate the relative yield and rise time of any Q_A^- formed under infrared conditions, we have monitored the variable fluorescence yield from PSII (Fig. 2). Fluorescence measurements give an alternate method of monitoring the Q_A oxidation state (see discussion in Ref. [70]). As Q_A is a fluorescence quencher, chlorophyll fluorescence is low (F_{eq}) in the dark. Charge separation occurs upon photoexcitation, and chlorophyll fluorescence increases as an equilibrium state of

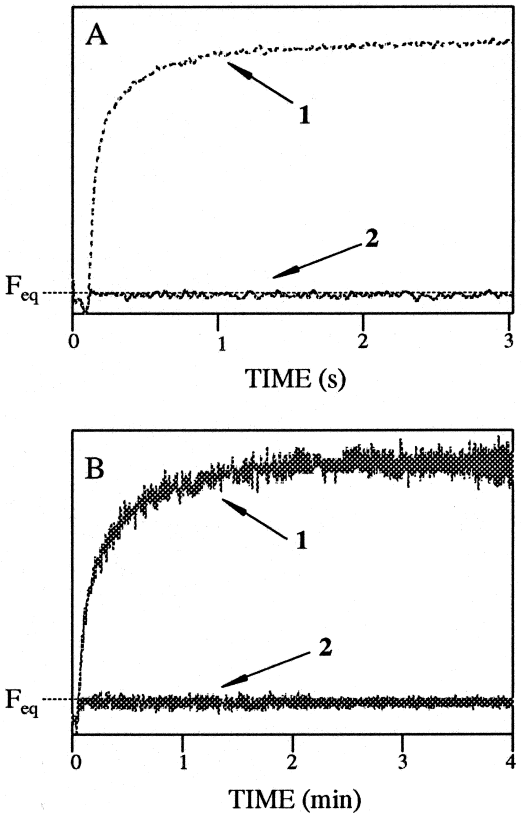

Fig. 2. Fluorescence yield in wildtype *Synechocystis* PSII preparations at pH 7.5. Partially dehydrated oxygen evolving PSII with 3 equivalents ferricyanide (trace 1) and manganese-depleted PSII with 3 mM ferricyanide and 3 mM ferrocyanide (trace 2) samples, identical to the samples used for FT-IR experiments, were continuously illuminated at −9°C for (A) 3 s and (B) 4 min. Samples used in (A) and (B) contained 40 and 25 μg chl, respectively. Spectra were corrected for differences in reaction center concentration. Data were obtained at −9°C.

$P_{680}Q_A^-$ is produced. While the positive control, identical to the above EPR control sample, shows a fluorescence yield increase under constant illumination at −9°C, consistent with reduction of Q_A (Fig. 2, line 1), no increase over F_{eq} is observed in manganese-depleted PSII in the presence of potassium ferri/ferrocyanide with either a 3 s (Fig. 2A, line 2) or a 4 min (Fig. 2B, line 2) illumination time.

In agreement with the EPR control experiments described above, the results of these fluorescence measurements allow us to conclude that there is no detectable Q_A^- formed under the conditions employed for infrared spectroscopy in cyanobacterial PSII; instead, potassium ferricyanide is reduced to form potassium ferrocyanide.

3.3. *Difference FT-IR spectra of tyrosyl radicals using continuous illumination*

Difference infrared spectra of tyrosine Z and of tyrosine D can be acquired by a series of data acquisitions on a single PSII sample using continuous illumination (Fig. 3A). A light-minus-*long* dark spectrum, reflecting Z•D•–Z D, can be constructed with a 90 min dark adaptation between a 4 min light and a 4 min dark spectrum. A light-minus-*short* dark spectrum, reflecting Z•–Z, can be constructed with a 4 min dark adaptation between the light and dark spectrum, which will not contain a large contribution from D•–D. The two difference spectra are recorded as alternate spectral collections on the same sample. Construction of the *double*-difference spectrum (Fig. 3A) emphasizes the contributions from the stable tyrosine radical. Unique vibrational modes of the tyrosyl radical will generate positive contributions to the spectrum, whereas unique vibrational modes of

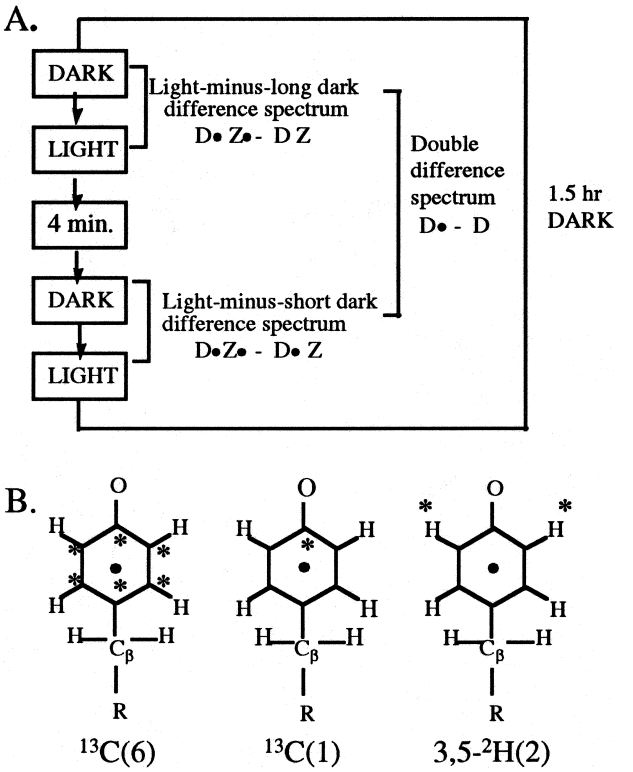

Fig. 3. (A) Schematic of difference FT-IR data collection method for Z•–Z and D•–D by continuous illumination at −9°C. The boxes labeled 'light' and 'dark' correspond to 4 min of data acquisition. (B) Structures of isotopically labeled tyrosines. Asterisks mark the ^{13}C or the ^2H on the tyrosine.

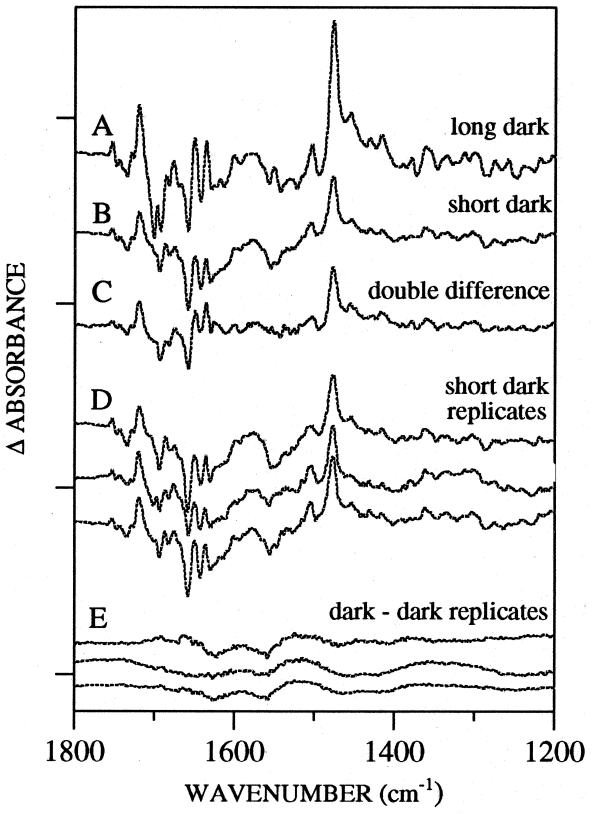

Fig. 4. Difference infrared spectra of manganese-depleted wild-type *Synechocystis* PSII preparations at pH 7.5. The (A) light-minus-long dark, (B) light-minus-short dark, and (C) double-difference infrared spectra shown were obtained using continuous illumination, according to the data acquisition methods described in Fig. 3A. Spectra in (A–C) are an average of 17 spectra. Three individual light-minus-dark difference spectra, taken from three different samples on three different days, are shown in (D). The corresponding three individual dark-minus-dark difference spectra are shown in (E). The tick marks on the *y* axis measure 5×10^{-4} absorbance units. Data were obtained at −9°C.

the neutral tyrosine will generate negative contributions.

The acceptor side will be reoxidized by a ferricyanide/ferrocyanide couple present in all infrared samples and makes no detectable contribution under these experimental conditions (see control experiments above). Ferricyanide and ferrocyanide exhibit characteristic ν(CN) absorptions at approximately 2112/2036 cm^{-1} [71], consistent with light-dependent oxidation and reduction of these compounds [51]. A light-minus-long dark (Fig. 4A), a light-minus-short dark (Fig. 4B), and a double-difference (Fig. 4C) spectrum with sufficient signal-to-noise ratio to discern all spectral features are constructed from each set. Difference and double-difference spectra were reproducible in intensity and frequency from sample to sample. Representative, individual difference spectra from wildtype, cyanobacterial PSII are shown in Fig. 4D; the three replicates were taken from three different samples on three different days of data acquisition. Multiple spectra are then averaged to achieve a good signal-to-noise ratio. Dark-minus-dark spectra do not exhibit discernible spectral features, as shown in three individual dark-minus-dark spectra (Fig. 4E). The intensity of red- and heat-filtered light used for 4 min illumination is low (see Section 2); the data in Fig. 4 show that 4 min illumination under these conditions has no deleterious effects on the PSII sample and results in reproducible spectra.

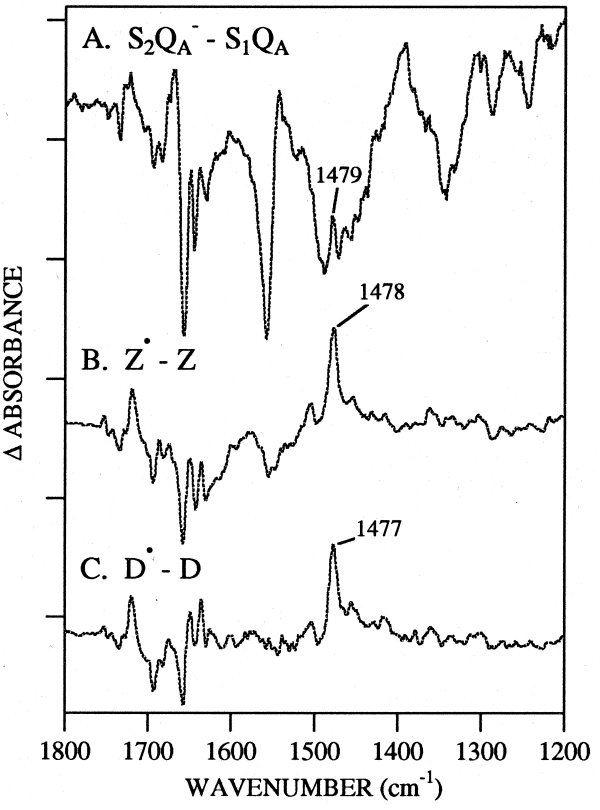

Fig. 5. Difference infrared spectra of *Synechocystis* PSII preparations. The difference spectra are of (A) $S_2Q_A^-$–S_1Q_A from oxygen-evolving cyanobacterial PSII, and (B) Z•–Z and (C) D•–D from manganese-depleted cyanobacterial PSII. Data shown in (A) are the average of 2 spectra; data shown in (B–C) are the average of 17 spectra. The tick marks on the *y* axis correspond to 2×10^{-4} absorbance units.

3.4. Comparison of difference FTIR spectra of $S_2Q_A^-$–S_1Q_A and of D•–D and Z•–Z

In Fig. 5A, we present data acquired at 200 K on manganese containing cyanobacterial PSII preparations, which contain one molar equivalent of potassium ferricyanide. Previous experiments [64] have shown that the reduced form of Q_A *is stably generated* under these conditions; these conditions are equivalent to those used to acquire the EPR spectra shown in Fig. 1B. The data in Fig. 5A demonstrate that spectra acquired under these conditions, corresponding to the maximum possible yield of Q_A^-, have little intensity in the 1479 cm^{-1} region. Remaining intensity in this region in Fig. 5A has been attributed to 0.3 spin chl^+ per reaction center, which is produced in this preparation upon illumination at 200 K [64].

On the other hand, as discussed above, when manganese-depleted, cyanobacterial PSII preparations containing 3 mM potassium ferricyanide and 3 mM ferrocyanide are emp1oyed, Q_A is not stably reduced at −9°C. Under these conditions, the intensity of the 1478/1477 cm^{-1} line increases in both the light-minus-short dark difference spectrum, ascribed to Z•–Z (Fig. 5B), and the double-difference spectrum, ascribed to D•–D (Fig. 5C).

The *inverse correlation* between the intensity of the 1478 cm^{-1} line and the amount of reduced Q_A argues against the assignment of the 1478/1477 cm^{-1} line to the C–O vibration of semiquinone anion Q_A^-. Vibrational lines of Q_A in Fig. 5A must be identified by isotopic labeling of plastoquinone; these experiments are in progress.

3.5. Effect of isotopically labeled tyrosines on the infrared spectra of tyrosyl radicals in PSII

Initial assignment of bands or lines in difference FT-IR spectra is usually performed by comparison to model compounds or by group frequency assignments. However, the protein environment may alter vibrational frequencies (see, for example Ref. [72]); therefore, group frequency assignments may be erroneous, when applied to the in vivo situation. Assignment of biological vibrational lines to a chemical group, i.e., tyrosine or quinone, requires isotopic labeling.

Isotopomers of tyrosine can be incorporated into cyanobacterial wildtype cells [28], thereby isotopically labeling all tyrosines in PSII. Three different isotopomers of tyrosine were utilized (Fig. 3B): (1) $^{13}C(6)$-tyrosine, in which all six ring carbons are labeled, (2) $^{13}C(1)$-tyrosine, in which C4, bound to the phenolic oxygen, is labeled, and (3) 3,5-$^{2}H(2)$tyrosine, in which ring carbons 3 and 5 are deuterated. Note that $^{13}C(6)$-labeling broadens the EPR spectra of both tyrosyl radicals (data not shown) and that tyrosine labeling does not result in isotopic incorporation, under these conditions, into plastoquinone or chlorophyll [28,49].

We will focus on the 1530–1370 cm^{-1} region of the FT-IR difference spectra of PSII; in Fig. 6A, we highlight this region of the Z•–Z spectrum, which is repeated from Fig. 5B. Unique vibrational modes of Z• make positive contributions to the spectrum; unique vibrational modes of Z make negative contributions. In Fig. 6B, we present the effect of hydroxylamine upon the infrared spectrum attributed to Z•–Z. This treatment blocks oxidation of tyrosine Z, but allows electron transfer from P_{680} to Q_A [73,74]. Previous work from our group has shown that an EPR signal from an oxidized chlorophyll can be detected in a small percentage of centers in the presence of this compound [49]. Fig. 6B shows that the intensity of the line at 1478 cm^{-1} decreases upon this treatment. Remaining intensity is ^{15}N sensitive and has been assigned to a chlorophyll cation radical, produced in a minority of centers [49].

Upon labeling all six ring carbons of tyrosine in PSII, the intensity of the positive line at 1478 cm^{-1} in the Z•–Z difference spectrum decreases and apparently downshifts to 1423 cm^{-1} (Fig. 6C); a new positive line at 1380 cm^{-1} also appears. A percentage of the original intensity remains at 1478 cm^{-1} upon $^{13}C(6)$ labeling. The amplitude of this remaining 1478 cm^{-1} line is similar to the amplitude remaining in the presence of hydroxylamine (compare Fig. 6B and C). We attribute this remaining intensity either to a chlorophyll cation radical, produced in the minority of centers, or to an oxidation-induced shift in the vibrational spectrum of chlorophyll. Oxidation effects (or electrochromic shifts) on the absorption spectra of photosynthetic pigments are well known (reviewed in Ref. [75]).

When $^{13}C(1)$-tyrosine labeling is employed, the

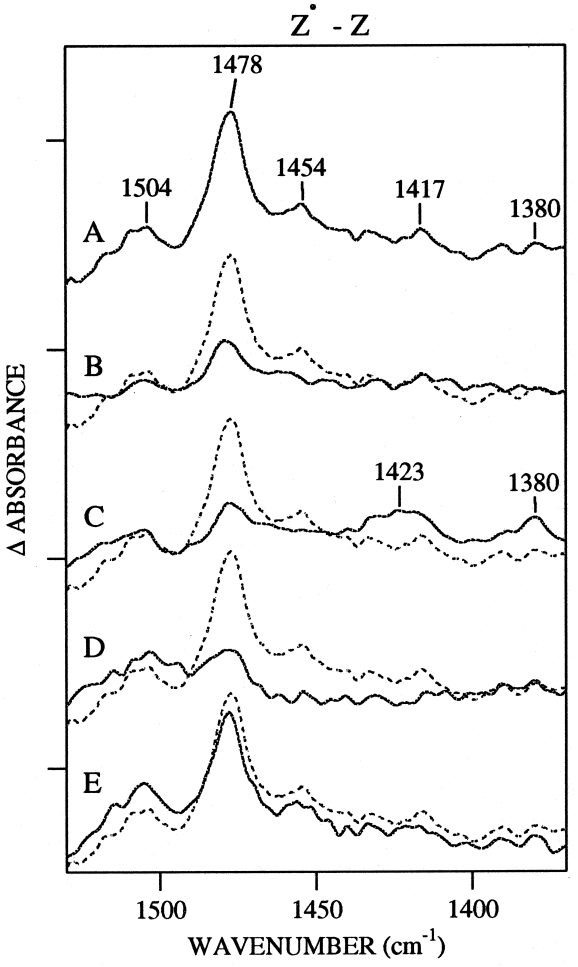

Fig. 6. Difference infrared spectra of Z•–Z from isotopically labeled, manganese-depleted *Synechocystis* PSII preparations at pH 7.5. The wildtype spectrum for Z•–Z is shown in a solid line (A) and is superimposed as a dashed line in (B–E). The Z•–Z spectra shown in solid lines were obtained from PSII samples containing: (B) hydroxylamine, (C) ^{13}C(6) labeled tyrosine, (D) ^{13}C(1) labeled tyrosine, and (E) 3,5-^{2}H(2) labeled tyrosine. The data shown were obtained using continuous illumination and are the average of 11–17 spectra. The tick marks on the *y* axis correspond to 2.0×10^{-4} absorbance units. Data were obtained at −9°C.

positive line at 1478 cm^{-1} in the Z•–Z spectrum decreases in intensity (Fig. 6D), equivalent to the effect of ^{13}C(6)-tyrosine labeling (Fig. 6C) and of hydroxylamine (Fig. 6B); the location of the downshifted line is not observable. This is common in difference infrared spectroscopy, where the location of downshifted lines is not always determinable (for example, see Refs. [39,76,77]). An approximately 40 cm^{-1} ^{13}C(6) downshift is expected from density functional calculations [78]. There is no significant alteration in the difference spectrum associated with Z•–Z between 1530–1370 cm^{-1}, when tyrosine is 3,5-deuterated (Fig. 6E). These data argue that the positive 1478 cm^{-1} vibration involves a C–O stretching mode of tyrosyl radical in PSII, as it is affected by both the exclusive labeling of the carbon bound to the phe-

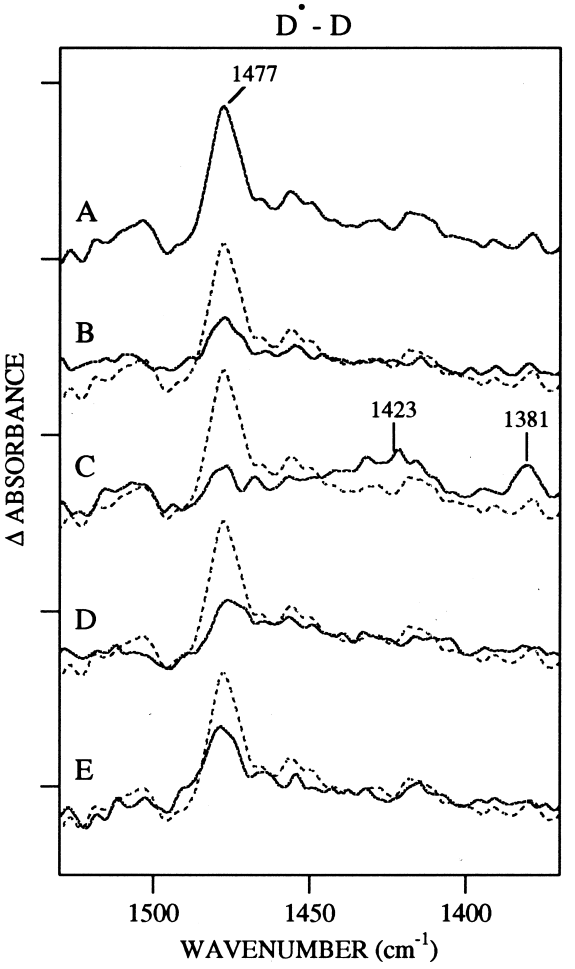

Fig. 7. Difference infrared spectra of D•–D from isotopically labeled, manganese-depleted *Synechocystis* PSII preparations at pH 7.5. The wildtype spectrum for D•–D is shown in a solid line (A) and is superimposed as a dashed line in (B–E). The D•–D spectra shown in solid lines were obtained from PSII samples derived from or containing: (B) YF160D2, (C) ^{13}C(6) labeled tyrosine, (D) ^{13}C(1) labeled tyrosine, and (E) 3,5-^{2}H(2) labeled tyrosine. The data shown were obtained using continuous illumination and are the average of 12–17 spectra. The tick marks on the *y* axis correspond to 2.0×10^{-4} absorbance units. Data were obtained at −9°C.

nolic oxygen and labeling of all ring carbons, but not by deuterium labeling at C3 and C5 of the tyrosine ring.

In Fig. 7A, we show the 1530–1370 cm^{-1} region of the double-difference D•–D infrared spectrum, obtained at pH 7.5. Unique vibrational modes of D• make positive contributions to the spectrum; unique vibrational modes of D make negative contributions. The tyrosyl D• radical in PSII exhibits pH dependent changes in this region; at pH 6.0, additional D• intensity is observed at 1473 cm^{-1} (data not shown) [27,48]. Data for D• are of lower signal-to-noise ratio, when compared to Z•, since *double-difference* spectra are employed. The YF160D2 mutant was used as a negative control. Although the EPR signal of D• is absent in the mutant, cells and PSII particles from this mutant are active in oxygen evolution, and light-driven electron transfer reactions can occur, involving P_{680}, Z, and Q_A [29,30,34]. Under illumination, the YF160D2 mutant exhibits a narrow, dark-stable EPR signal in a minority of centers, which may be from a chlorophyll radical [29,30,34].

When PSII is isolated from the YF160D2 mutant, in which tyrosine D is replaced by a nonredox-active phenylalanine, the intensity of the 1477 cm^{-1} line decreases in the D•–D spectrum (Fig. 7B), as expected if this vibrational mode arises from D•. The remaining intensity may be due to a small chlorophyll radical contribution to the spectrum, or oxidation of tyrosine D may change the vibrational spectrum of chlorophyll through an electrostatic effect. Given the signal-to-noise ratio, the effects of incorporation of these three different isotopomers on the difference infrared spectrum associated with D•–D (Fig. 7C–E) appear to be similar to those described above for Z•–Z. Note that remaining intensity at 1477 cm^{-1}, after isotopic labeling, is similar to the remaining intensity observed in the YF160D2 mutant (Fig. 7B), which lacks D• entirely. A line at 1504 cm^{-1} is observed in both D•–D and Z•–Z spectra; the intensity of this line is not dramatically affected by isotopic labeling of tyrosine (Figs. 6 and 7).

These isotopic labeling experiments cumulatively argue that the positive 1478 and 1477 cm^{-1} modes may be assigned to a vibrational mode involving a ν(C–O) stretch of tyrosyl radicals, Z• and D•, respectively, in PSII.

3.6. Control EPR experiments for difference FT-IR measurements, employing flash illumination

EPR characterization of Z• and D• decay kinetics in spinach, OGP-derived, PSII core samples, containing 3 mM ferricyanide and 3 mM ferrocyanide, was performed. Fig. 8A (solid line) shows the composite tyrosyl Z• and D• spectrum, generated under continuous illumination. Upon 42 s of dark adaptation (Fig. 8A, dotted line), the fast decrease in signal amplitude following illumination represents the decay of tyrosyl Z• radical in the dark; the remaining signal arises solely from the tyrosyl D• radical. The subsequent decrease in signal amplitude after 10 min dark adaptation is indicative of the slow decay of tyrosyl D• radical (Fig. 8A, dashed line).

Fig. 8B and C show the decay of kinetic transients on two different time scales. Kinetic transients were recorded with saturating laser flashes (Fig. 8B and C) and at a constant magnetic field, which monitors the amplitude of the low-field shoulder (see arrow in Fig. 8A) in the Z• and D• EPR signals. The fast (Fig. 8B) and slow (Fig. 8C) components represent mainly the decay of tyrosyl Z• and tyrosyl D• radical, respectively. Analysis of the data shows that, in this preparation, the decay of Z• is biexponential. The overall lifetime ($t_{1/2} = 250$ ms) is in agreement with other measurements of Z• decay in Tris-washed spinach and cyanobacterial PSII [79]. The time between the flashes was 5 s; this is sufficiently short that the slowly decaying D• radical (see Fig. 8C) will not make a dominant contribution to the kinetic trace.

Kinetic data were obtained on tyrosyl D• decay following eight saturating flashes (Fig. 8C). The decay of tyrosyl Z• may make a contribution to the very early phase of the measured decay, but it is not a large contribution since the Z• signal has decayed to a nondetectable level in 500 ms after the flash (see Fig. 8B). Fig. 8C shows that the decay of D• is biphasic, with a fast and slow phase. For this transient, $t_{1/2}$ equals 26 s. The rates of tyrosyl D• radical decay are faster in this particular spinach core preparation, which is isolated with OGP, when compared to others previously characterized [47,53,57]. Kinetic data were also obtained on tyrosyl D• decay using single flashes every 132 s (Fig. 8D). This is a data acquisition method that directly corresponds to the method of FT-IR data acquisition,

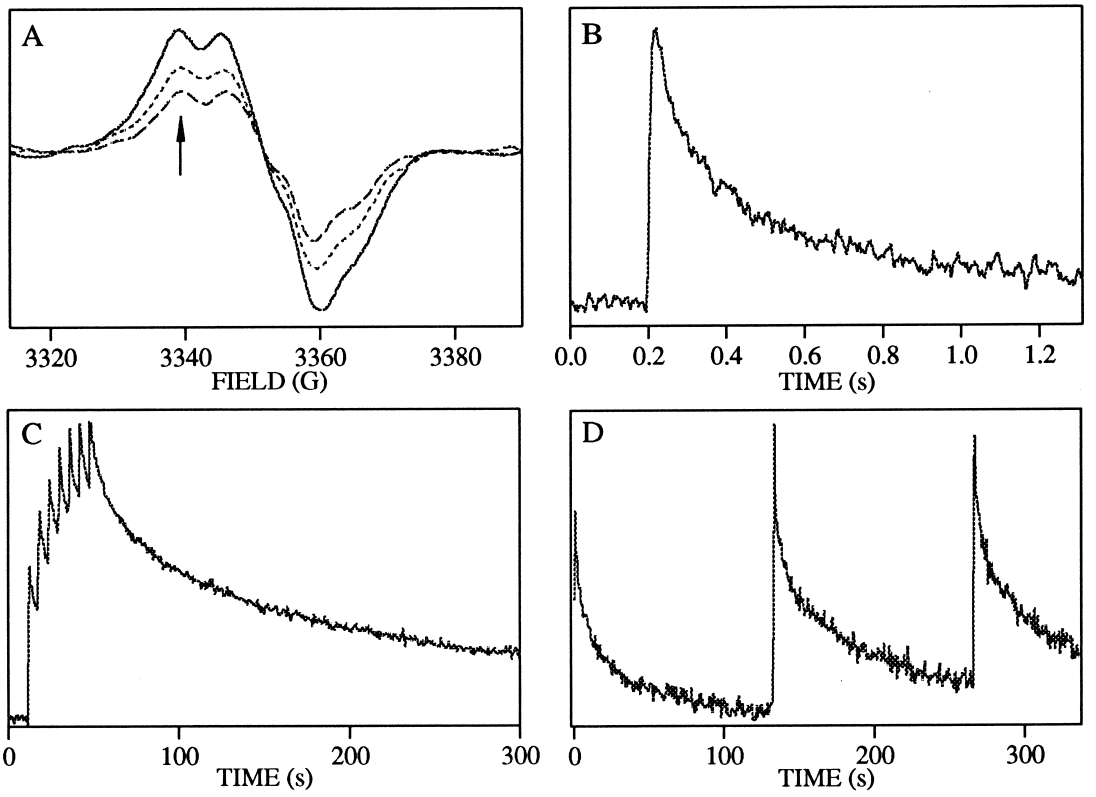

Fig. 8. EPR controls for difference FT-IR measurements using flash illumination. (A) Tyrosyl spectra generated using continuous illumination (solid line), 42 s dark adaptation (dotted line), and 10 min dark adaptation (dashed line). Manganese-depleted spinach core PSII samples contained 80 μg chl. (B) Decay kinetics of tyrosyl Z• radical in manganese-depleted spinach core PSII preparations. The sample contained 160 μg chl. Spectra shown are an average of 50 flashes at a repetition rate of 0.2 Hz. (C) Decay kinetics of tyrosyl D• radical in manganese-depleted spinach core PSII preparations. The sample, which contained 160 μg chl, was photoexcited by 8 consecutive flashes and the decay was monitored for 10 min. (D) Decay kinetics of tyrosyl D• radical in manganese-depleted spinach core PSII preparations. The sample, which contained 160 μg chl, was photoexcited by 1 flash every 132 s. Data were obtained at −10°C.

described below. Kinetic data were obtained in the presence and absence of 100 μM DCMU; these experiments showed that the decay of D• was not altered by the presence of this inhibitor (data not shown). We therefore conclude that D• is not decaying by recombination with Q_B^-.

3.7. *Control fluorescence experiments for difference FT-IR measurements, employing flash illumination*

The fluorescence decay kinetics of Q_A^- in this spinach OGP preparation were monitored using pulsed illumination (Fig. 9). Reoxidation of Q_A^- by charge recombination or by exogenous acceptors will result in time-dependent decreases of chlorophyll fluorescence intensity [70]. In contrast to cyanobacterial PSII (Fig. 2), the spinach OGP preparation, in the presence of 3 mM potassium ferricyanide and 3 mM potassium ferrocyanide, exhibits detectable fluorescence (Fig. 9, line 2). The fluorescence yield is reduced by approximately 50% when compared to the control, which is manganese depleted and contains only one equivalent potassium ferricyanide (Fig. 9A, line 1). The fluorescence transient, obtained in the presence of 3 mM potassium ferricyanide and 3 mM potassium ferrocyanide, decays to baseline in approximately 1 s after illumination (Fig. 9B, line 2). The decay time of the fluorescence transient was not altered in the presence of 100 μM DCMU (data not shown). The 400 ms pulse of modulated actinic light is the shortest interval allowable on the instrumentation used; this is the closest approximation of the flash illumination utilized for infrared data acquisi-

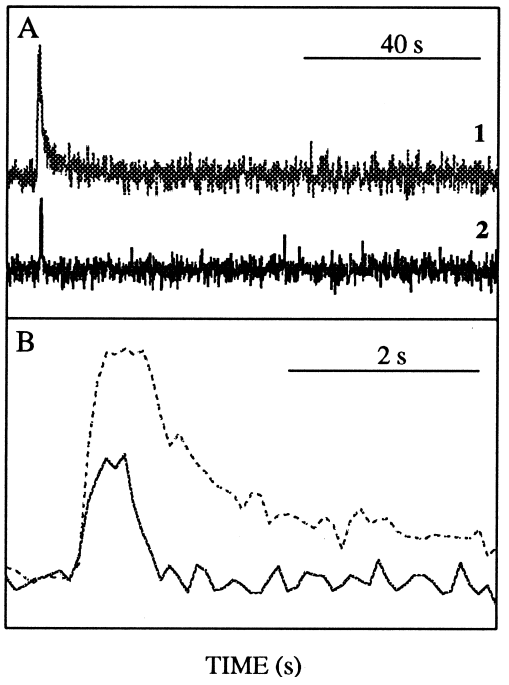

Fig. 9. (A) Fluorescence transient in manganese-depleted spinach OGP PSII preparations at pH 7.5. Samples contained either one equivalent (trace 1) or 3 mM potassium ferricyanide and 3 mM potassium ferrocyanide (trace 2). (B) Expanded view of the transients shown in (A). Data were obtained at −10°C.

tion (laser flash and <0.7 s before data acquisition) available to us at this time. A modulated fluorometer has a monitoring beam with a small actinic effect, which will 'close' reaction centers and which will bias the kinetics toward slightly faster rates [70]. However, the positive controls, obtained either on the manganese-depleted OGP preparation (Fig. 9A, line 1; and B, dotted line) or on an oxygen evolving preparation (data not shown), in the presence of only one equivalent potassium ferricyanide, demonstrate that we can detect slow components in the fluorescence decay using this experimental setup. Thus, the results of kinetic fluorescence measurements allow us to argue that, under the conditions employed and in this OGP spinach preparation, any Q_A^- produced decays completely in 1 s after a saturating flash.

3.8. *Difference FT-IR spectra of tyrosyl radicals using flash illumination*

Difference infrared spectra were acquired on PSII samples using flash illumination (Fig. 10, panel I). Two interferograms were recorded sequentially in the dark before illumination (D1 and D2); two interferograms were recorded sequentially (L1 and L2) after the laser flash (Fig. 10, panel I); this series was iterated. The total time between the laser flashes was 132 s, and a preflash was given 132 s before the beginning of data acquisition.

Fig. 10, panels II and III, show difference infrared spectra, constructed from four 33 s data sets, to give L1/D2 (Fig. 10A and a), L2/D2 (Fig. 10B and b), and D1/D2 (Fig. 10C and c). All spectra in Fig. 10 are corrected for a 0.35 amide II absorbance and are presented on the same y scale. EPR control experiments show that the tyrosyl D• radical will decay by 64% in 132 s and thus should contribute to the difference infrared spectra. As shown above, the tyrosyl Z• radical decays (<0.7 s) before the beginning of data acquisition and will not make a large contribution to the spectrum. Also, we have shown that any Q_A^- produced decays within 1 s after illumination. Thus, the time evolution of the difference infrared spectra over 132 s (Fig. 10A–C) should reflect only the decay of tyrosyl radical D•. Vibrational modes of the tyrosyl radical will generate positive lines in the spectrum, and vibrational modes of the neutral tyrosine will generate negative lines.

The FT-IR spectra, constructed from these sequential 33 s data sets, exhibit a 1477 cm^{-1} line (Fig. 10, Panel II). As time elapses after the flash, the amplitude of the 1477 cm^{-1} line decreases (Fig. 10, Panel III). This time-dependent decrease in the amplitude of the 1477 cm^{-1} line, after flash illumination, qualitatively correlates with the decay behavior of the tyrosyl D• radical, as evidenced by EPR spectroscopy (Fig. 8C and D). The L1/D2 and L2/D2 spectra show a differential feature in the 2200–2000 cm^{-1} region due to redox changes involving potassium ferricyanide and potassium ferrocyanide (data not shown). This feature decreases in intensity with time. Difference infrared spectra were also constructed from four 5.8 s data sets recorded immediately after flash illumination (data not shown); these data give similar results.

To yield a quantitative comparison of the decay of the species monitored via EPR spectroscopy and via the 1477 cm^{-1} infrared absorption, we present the graph in Fig. 11. For the difference infrared data, acquired with both 33 s intervals, the amplitude of

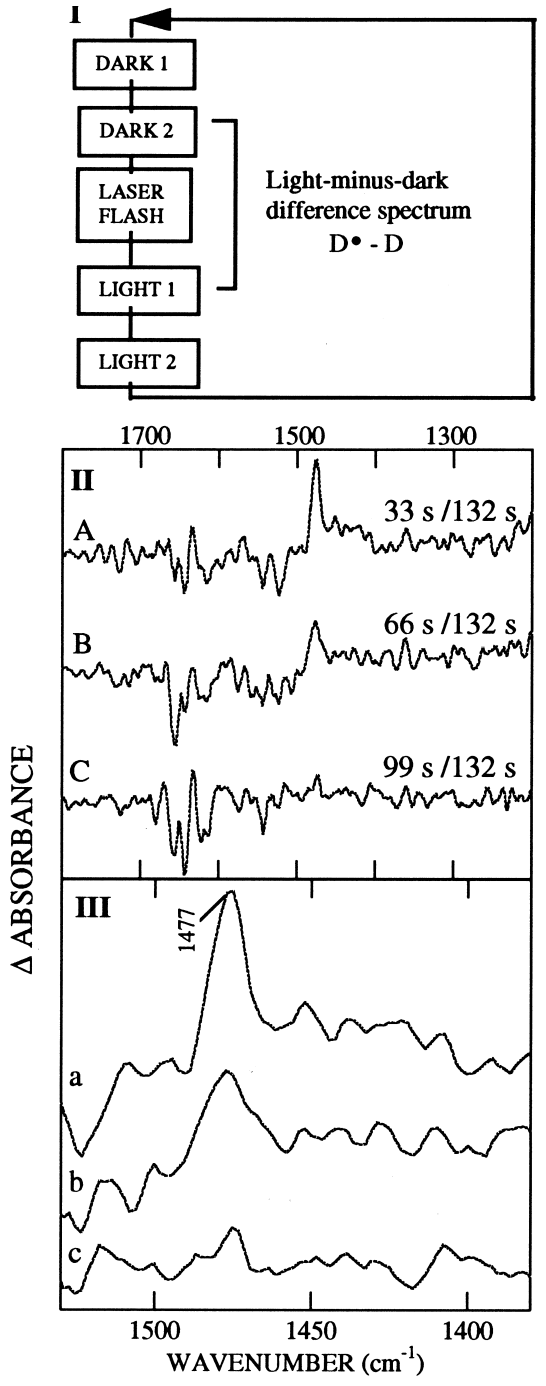

Fig. 10. (I) Schematic of difference FT-IR data collection method reflecting D•–D, as a function of time after a single saturating flash at −10°C. Boxes, L1, L2, D1, and D2 correspond to 33 s of data acquisition. There was no dark delay between L2 and D1. (II) Decay of D•, as assessed by difference infrared spectroscopy, in manganese-depleted spinach OGP PSII preparations at pH 7.5. Data were acquired in 33 s intervals for 132 s after the flash. The D•–D spectra from PSII samples were constructed from (A) 0–33 s/100–132 s (L1/D2); (B) 34–66 s/100–132 s (L2/D2); and (C) 67–99 s/100–132 s (D1/D2). (III) Difference infrared spectra of D•–D, repeated from panel (II), showing the 1530–1380 cm^{-1} region. Spectra were acquired in series from a PSII sample and are the average of 50 data sets per sample. Spectra were obtained at −10°C.
←

the 1477 cm^{-1} line was measured for each time point; each amplitude was normalized by the sum of the measured amplitudes. The resulting data are plotted versus time (Fig. 11, circles). The EPR decay (Fig. 8C and D) was integrated from 0–33, 34–66, and 67–99 s; the integrated area from 100–132 s was subtracted from each of the above integrated areas. The resulting values were normalized by the sum; these values correspond to the percent of D• decay, as assessed by EPR spectroscopy, in each time period. These data are plotted as a function of time (Fig. 11, squares and triangles). There was no significant difference when EPR data were obtained from either multiple flashes (Fig. 11, triangles) or from single flashes separated by 132 s (Fig. 11, squares).

Fig. 11 shows that, within the signal-to-noise ratio of the two measurements, the decay of the 1477 cm^{-1}

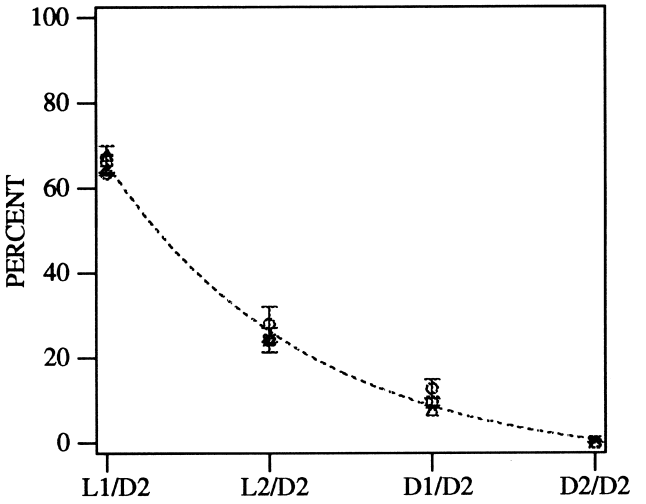

Fig. 11. Decay of tyrosyl D• signals, as assessed by EPR and difference FT-IR spectroscopy, in manganese-depleted spinach PSII preparations. Data plotted are from flash illumination infrared measurements, shown in Fig. 10 (circles). Also plotted are the corresponding, integrated areas from the kinetic EPR decay of tyrosyl D• radical, shown in Fig. 8C (triangles) and Fig. 8D (squares). The best fit to the data points is shown as the dotted line.

line parallels the decay of the tyrosyl D• EPR signal, when 33 s intervals between flashes are used. Integrated EPR and FT-IR data, using 5.8 s intervals between flashes, plotted as a function of time, gave similar results (data not shown). Superposition of the kinetic data provides strong support for the assignment of the observed 1477 cm^{-1} line to the tyrosyl D• radical.

3.9. EPR spectra obtained in phosphate/formate containing buffers

An alternative spectrum, assigned to D•–D, has been described [45,46]. This alternative spectrum lacks a 1477 cm^{-1} line and has been obtained on spinach PSII membranes and a cyanobacterial core PSII preparation [45,46]; observation of this spectrum seems to be dependent on the use of high concentrations of phosphate/formate/potassium ferricyanide. In Fig. 12, we present EPR data obtained on spinach PSII membranes under our conditions (5 mM HEPES-NaOH, pH. 7.5, 3 mM potassium ferricyanide, and 3 mM potassium ferrocyanide (Fig. 12, dashed line)) and on spinach PSII membranes under the conditions employed in Refs. [45,46] (50 mM sodium phosphate, pH 6.0, 50 mM sodium formate, 10 mM NaCl, 15 mM $MgCl_2$, and 64 mM potassium ferricyanide (Fig. 12, solid line)). Both samples were preilluminated before the beginning of data acquisition. The samples in phosphate/formate buffers show the reported increase in the rate of decay of D• (data not shown) and the reported accumulation of a narrow radical, which distorts the tyrosyl radical spectrum at g=2 (Fig. 12, solid line) [45].

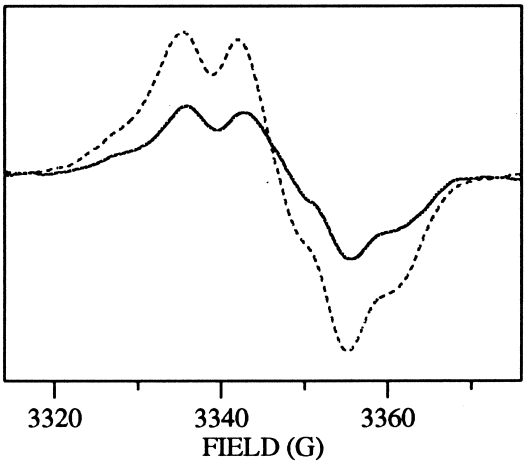

Fig. 12. EPR spectra of tyrosyl radicals. Spectra were obtained from manganese-depleted spinach PSII membranes resuspended in 5 mM HEPES-NaOH, pH 7.5, 3.0 mM potassium ferricyanide, and 3.0 mM potassium ferrocyanide at 3.4 mg chl/ml (dashed line) and 50 mM sodium phosphate pH 6.0/50 mM sodium formate/64 mM potassium ferricyanide at 3.7 mg chl/ml (solid line). Spectra were recorded from 0–42 s after illumination and were acquired at −9°C. Spectra are corrected for the difference in protein concentration.

Fig. 12 presents the yield of tyrosine D• obtained 0–42 s after illumination. Spin quantitation shows that the D• EPR spectrum, obtained in the presence of phosphate/formate (Fig. 12, solid line), is 50% of the D• EPR spectrum, obtained in the presence of HEPES (Fig. 12, dashed line). The spectra obtained under illumination gave a similar result (data not shown). The spectra in Fig. 12 were obtained on aqueous samples; partially dehydrated samples, containing phosphate/formate, gave an even lower yield of D•, when compared to HEPES-buffered samples (data not shown). We conclude that high phosphate/formate/ferricyanide conditions are not optimal for the observation of tyrosine D oxidation.

4. Discussion

Infrared spectroscopy is a powerful method for probing photo-induced structural alterations in PSII. Changes in hydrogen bonding, conformational changes, and electrostatic relaxations can be detected. In principle, all vibrational transitions of the entire PSII complex contribute to the FT-IR spectrum. Difference FT-IR spectroscopy permits measurement of absorbance differences on the order of 10^{-4} with a high signal-to-noise ratio and reproducibility. Vibrational lines of tyrosine and the tyrosyl radical can be observed. The difference spectrum originates in the changes in bond strength, which are expected upon oxidation of tyrosine [80]. Amino acid residues or pigments in the environment of the tyrosine may also contribute to the spectrum, if there are redox-linked structural changes, i.e., protonation, hydrogen bonding, electrostatic interactions, involving these species.

A debate in the literature has concerned the assignment of the positive band at 1478/1477 cm^{-1}. Past assignments of components of this line include

tyrosyl radicals, Q_A^-, and a chlorophyll cation radical [27,42–46,49,51,81]. Our experiments in this paper are designed to address this controversial topic.

4.1. Summary of EPR and fluorescence experiments

We have presented difference FT-IR spectra, acquired using continuous illumination, associated with the oxidation of tyrosine Z and of tyrosine D in PSII. As a control for our infrared data, EPR measurements, using identical illumination regimes, were performed on PSII samples, which are biochemically identical to those used for difference FT-IR measurements. No detectable $Fe^{2+}Q_A^-$ signal is observable in cyanobacterial PSII by EPR techniques, under the conditions used for infrared spectroscopy. Note, that for cryogenic EPR measurements, the photo-induced equilibrium state is trapped by freezing in liquid nitrogen. A cryogenic EPR spectrum of an illuminated PSII sample is a representation of a trapped radical state, whereas an infrared spectrum, recorded under continuous illumination, is a time-averaged representation of the radical state. Therefore, as an additional control, fluorescence measurements were employed. These experiments confirm that the equimolar mixture of potassium ferrocyanide and ferricyanide prevents the detectable reduction of Q_A in cyanobacterial PSII. Fluorescence spectroscopy has the advantage that the timescale of the measurement is more similar to the infrared time scale. Because infrared data obtained under these conditions exhibit an intense 1478/1477 cm^{-1} line, this set of experiments argues against the assignment of these spectral features to Q_A^-.

4.2. Infrared spectroscopy on isotopically labeled PSII

Examination of three cyanobacterial samples in which tyrosine, but not plastoquinone or chlorophyll [27,28], is isotopically labeled, allows assignment of the 1478 and 1477 cm^{-1} lines to a vibrational mode involving the C–O stretching vibration of tyrosyl radicals, Z• and D•.

Upon labeling of tyrosine with ^{13}C at all six ring positions, the 1478 cm^{-1} line in the Z•–Z difference spectrum decreases in intensity and apparently downshifts to 1423 cm^{-1} (Fig. 6C); a new positive line at 1380 cm^{-1} also appears. A percentage of the original intensity remains at 1478 cm^{-1} upon $^{13}C(6)$ labeling. The amplitude of this line is similar to the amplitude remaining in the presence of hydroxylamine. The 55 cm^{-1} downshift, observed upon $^{13}C(6)$-tyrosine labeling, argues that ring carbons of the tyrosyl radical contribute to the 1478 cm^{-1} line. $^{13}C(1)$ labeling, at the carbon bonded to the phenol oxygen, also results in a decrease in the intensity of the 1478 cm^{-1} line, although the position of the downshifted line could not be identified in the difference spectrum. However, ^2H labeling at the C3 and C5 positions does not result in a significant alteration in the 1478 cm^{-1} spectral feature. Taken together, these results are consistent with a significant ν(C–O) stretching displacement contributing to the 1478 cm^{-1} feature [78,80,82,83]. Similar results, given the lower signal-to-noise ratio, were obtained for tyrosine D•. Contrary to expectations developed from phenoxyl and tyrosine model compounds in vitro [78,80,82,83], this result suggests that the C–O stretching vibration of PSII tyrosyl radicals at pH 7.5 is relatively isolated from the C–H motion of the ring. Not only is the normal mode character of this line altered from what is observed in vitro, but the frequency of this line is also approximately 30 cm^{-1} downshifted from the in vitro value. These perturbations of the normal modes of vibration could be related to the fact that the tyrosyl radicals in PSII are involved in a peptide bond, whereas the tyrosyl radicals in vitro were free in solution [78,80,82,83]. Normal coordinate calculations have not been performed for the peptide-bound radical [78,80,82,83]. Another possible explanation for the perturbations observed in vivo is that electric field effects shift the frequencies of these vibrational modes and thus change interaction terms.

A Fermi resonance of the 'C–O stretching' mode (ν7a) and a C–C ring stretch [78,83] may explain the appearance of the broadened, downshifted 1423 cm^{-1} and a second 1380 cm^{-1} line upon $^{13}C(6)$-labeling of tyrosine. However, no significant change is observed upon deuteration at the C3 and C5 positions. This result suggests that the additional vibrational mode, involved in a possible Fermi resonance, does not involve significant C–H displacements at C3 and/or C5. Ring stretching vibrations, such as ν19a and ν19b, are predicted to fall in the 1400 cm^{-1} region, making them candidate vibrations, but are also expected to show substantial downshifts upon

deuteration of the ring [78,80,82,83]. To explain our results, we again must postulate perturbations of the vibrational spectrum of tyrosyl radicals in vivo. The origin of these perturbations is under investigation.

These experiments, taken together, demonstrate that a component of the spectral feature at 1478/1477 cm^{-1} arises from cyanobacterial D• and Z• and that this normal mode involves significant ν(C–O) stretching character. Our results argue against the conclusion [44] that the entire 1478/1477 cm^{-1} feature in our infrared spectra arises from Q_A^-.

4.3. Infrared control experiments

Infrared spectra were obtained on cyanobacterial samples under conditions in which Q_A^-–Q_A contributes to the spectrum, but Z•–Z and D•–D do not [63,64]. This experiment supports the assignment of the 1478/1477 cm^{-1} lines to D• and Z•, but not to Q_A^-.

It is important to point out that difference infrared spectra may have contributions from other tyrosines, besides the redox-active tyrosine residues. For example, the vibrational spectra of tyrosines could reflect deprotonation/reprotonation or changes in hydrogen bonding (see, for example, Ref. [84]). Therefore, the negative control experiments reported here have been necessary in interpreting the difference infrared spectrum.

As a negative control for Z• formation, a light-minus-short dark difference spectrum was obtained on samples treated with hydroxylamine. Hydroxylamine blocks the oxidation of tyrosine Z and leads to the expected alterations in the difference Z•–Z infrared spectrum. As a negative control for D• formation, a double-difference infrared spectrum was obtained on PSII samples isolated from the YF160D2 mutant, which lacks tyrosine D. Again, the expected alteration in the difference D•–D infrared spectrum was observed. These experiments show that the amplitude of vibrational modes at 1478/1477 cm^{-1} is decreased in both negative controls, as expected if these 1478/1477 cm^{-1} features arise from Z• and D•.

4.4. Comparison and normalization of FT-IR data

The FT-IR data, obtained on negative controls and on isotopically labeled samples, were normalized using the total protein concentration and/or amide II band intensity for analysis. These methods, which are the basis for quantitative comparison of infrared spectra, gave equivalent results. Thus, the representation of FT-IR is similar to that employed for EPR spectroscopy. Furthermore, this method permits differentiation of vibrational modes between different PSII reaction centers, such as mutant and wildtype cyanobacterial PSII samples, based on functional capacity. We have found that normalization on the ferricyanide/ferrocyanide band, as performed in Ref. [77], is not as reliable a comparative method for infrared data. This method of normalization assumes that all PSII reaction centers are equal in ability to undergo charge separation; this assumption can be erroneous. Interactive subtraction methods, as a basis for comparison, are also not reliable, since the result may be biased by assumptions concerning the data.

4.5. Kinetic transients as measured by EPR and FT-IR spectroscopy

Results from the flash-induced FT-IR are particularly important, since, to our knowledge, this is the first time a quantitative comparison of kinetics has been used to assign a vibrational line in the PSII infrared spectrum. In our flash experiments, spectra were acquired for 33 s at four intervals following a single saturating flash. Data acquisition begins < 0.7 s after the laser flash; fluorescence controls show that Q_A^- makes no contribution 1 s following illumination. In this flash infrared experiment, the time-dependent decay of the 1477 cm^{-1} line over 33 s intervals parallels the decay of the tyrosyl D• EPR signal. This experiment lends strong support to the experiments described above and also supports our previous assignments of the 1478/1477 cm^{-1} line(s) to the tyrosyl radicals in spinach and cyanobacterial PSII [27,47–49,51].

4.6. Alternative assignment of the 1478 cm^{-1} line to Q_A^- [42]

The investigation described in Ref. [42] yields a difference FT-IR spectrum in which a 1478/1477 cm^{-1} line was obtained and attributed to the ν(C–O) stretch of semiquinone anion, Q_A^-. This as-

signment was made based on a study of spinach PSII membranes (approximately 270 chl per reaction center [52]), containing hydroxylamine and PMS, which were added as an electron acceptor. The basis for this assignment was: (1) an apparent lack of ^{15}N shift in the 1478/1477 cm^{-1} line in the presence of hydroxylamine [43,44], (2) an apparent lack of production of donor side signals in EPR control experiments [44]; and (3) the production of a $Fe^{+2}Q_A^-$ signal in EPR control experiments [44].

In previous work, we reproduced the data of Ref. [42], except for minor differences in the amide I region [49], by employing PSII membranes, containing hydroxylamine and potassium ferricyanide. Also, PSII complexes from spinach (120 chl per reaction center [52]) and cyanobacterial (56 chl per reaction center [52]) PSII were employed. Illumination conditions for the EPR and FT-IR experiments were identical, and samples were identical except for the identity of the solid substrate [49]. This study [49] showed that the 1478 cm^{-1} line produced in cyanobacterial PSII in the presence of hydroxylamine, was ^{15}N sensitive and exhibited a 2 cm^{-1} downshift; multiple repeats of this experiment gave identical results. Global ^{15}N labeling was performed by growth of cyanobacterial wildtype cultures in the presence of ^{15}N nitrate and verified to be greater than 90% by mass spectrometry [49]. We concluded that the 1478 cm^{-1} line, produced in the presence of hydroxylamine in cyanobacterial PSII, arises from a chlorophyll cation radical. In spinach PSII under these conditions, the concomitant production of a chlorophyll cation radical in a minority (5%) of centers was observed by EPR spectroscopy. Infrared control experiments showed that this amount of chlorophyll is detectable. These EPR control experiments were used to argue that the 1478 cm^{-1} line in spinach PSII also arises from a chlorophyll cation radical [49]. Overall, these results led us to the conclusion that hydroxylamine cannot be used to obtain a 'pure' Q_A^-–Q_A difference spectrum in either cyanobacterial and spinach PSII.

The conclusions of Ref. [44] contradict these deductions. However, in our view, these experiments [44] do not provide strong support for the assignment of the 1478/1477 cm^{-1} line, produced in spinach in the presence of hydroxylamine, to the C–O stretching vibration of Q_A^-.

First, ^{15}N labeling was not verified by mass spectrometry, but by ESEEM spectroscopy, which is not as accurate a measure of the amount of isotope incorporation. In mass spectroscopy, each isotopomer contributes to the spectrum with an intensity that is related to the concentration of that isotopomer. This allows the detection of small alterations in the amount of isotope incorporation without ambiguity. In addition, use of a eukaryotic, rather than a prokaryotic source, can decrease the extent of ^{15}N labeling. In plants, the presence of stored material in the seed can decrease the amount of isotope incorporation and the presence of organelles can lead to differences in the compartmentalization of isotopes. Since the expected ^{15}N vibrational shift is small, a small decrease in the amount of ^{15}N incorporation could make the isotope shift unobservable.

Second, the conditions used for the FT-IR measurements and the EPR control experiments were not identical [44] and, therefore, were not directly comparable. The FT-IR spectra were acquired at high chlorophyll concentrations with a saturating 532 nm laser flash. The EPR spectra were acquired with a 2 s broad band illumination with a white light source. At concentrations of 15 mg ml^{-1}, such a 2 s illumination may not produce the full amplitude of EPR signals. Supporting this interpretation, the magnitude of the iron-quinone signal, produced by the 2 s illumination, is small, based on the signal-to-noise ratio of the EPR spectrum [44]. Thus, the above reported experiments do not rule out a chlorophyll radical or D• radical contribution, which would be expected under the conditions employed [49]. Also, when the content of chlorophyll cation radicals was determined, instead of quantitating the EPR signal with a spin standard, spectra were normalized to a second PSII sample [44]. This procedure involves assumptions concerning similarity of the two samples and is not as accurate a representation of radical content, as reference to a spin standard [49]. Finally, a 12 s sweep time after illumination was employed in both FT-IR and EPR experiments [44]. Data acquisition is then not equivalent, since infrared data are recorded simultaneously, in the time domain, whereas EPR field swept data are recorded as a function of the magnetic field. For example, radicals decaying in 4 s would not contribute to the midfield region of the 12 s EPR spectrum, but would contribute to the 12 s

infrared spectrum. Thus, the failure to see donor side EPR contributions in the experiments of Ref. [44] could be caused by any of a number of experimental factors and does not permit the conclusion that there are no contaminating donor side radicals in the presence of hydroxylamine. Many of the concerns described here have been discussed previously [49].

4.7. An alternative spectrum has been assigned to D•–D [44,45]

An alternative difference infrared spectrum has been assigned to D•–D [44]. This spectrum lacks a 1477 cm^{-1} line. Observation of this spectrum appears to be dependent on the presence of high concentrations of phosphate, formate, and potassium ferricyanide in PSII samples (see also Ref. [46]). This spectrum resembles, but is not identical, to our flash data obtained 99 s after a saturating flash (Fig. 10C, D1/D2), i.e., after the decay of the 1477 cm^{-1} line arising from tyrosine D.

The alternative D•–D spectrum, obtained in the presence of phosphate/formate, was described first through the use of spinach PSII preparations [44]; in this work, the ν(C–O) mode is assigned to a positive 1504 cm^{-1} line, based on group frequency assignments. More recently, a difference infrared spectrum, assigned to D•–D, was obtained on a *Synechocystis* PSII non-oxygen evolving core preparation [45]; this spectrum also lacks a 1477 cm^{-1} line. Experiments were performed to investigate whether the 1503 cm^{-1} mode is affected by $^{13}C(6)$, $^{2}H(4)$, and $^{13}C(1)$ labeling of tyrosines. Direct comparison of the data showed a decrease in the intensity of the 1503 cm^{-1} (approximately 50%) upon incorporation of $^{13}C(1)$-labeled tyrosines into cyanobacterial PSII; a new, more intense positive line at 1476 cm^{-1} was observed. However, there was no significant intensity change, given the signal-to-noise ratio of the measurements, observable in the positive 1503 cm^{-1} line upon incorporation of $^{13}C(6)$- or $^{2}H(4)$-labeled tyrosines into cyanobacterial PSII, although a new positive line appears at 1468 and 1486 cm^{-1}, respectively. If the positive 1503 cm^{-1} line in the difference FT-IR spectrum arises from a C–O stretching vibration of the tyrosyl radical, the infrared data from PSII containing either $^{13}C(6)$- or $^{13}C(1)$-tyrosine would be expected to show a marked decrease in intensity. Note that the double difference spectra (control−minus−isotopically labeled PSII), which are reported in Ref. [45] do not closely resemble the direct comparison of the spectra [45]; the basis by which these double difference spectra were constructed is not clear.

Overall, in our view, from this set of infrared data on isotopically labeled PSII [45], the assignment of the 1503 cm^{-1} line in the alternative D•–D spectrum remains uncertain. Also, spectral shifts in this alternative D•–D spectrum, obtained in a mutant HQ189D2, do not alter regions of the spectrum affected by ^{13}C labeling of histidine [45]. This histidine 189 residue in the D2 polypeptide is in close proximity to and hydrogen bonds with tyrosine D; mutation of histidine 189 in D2 to a glutamine alters the environment of tyrosine D [24,37,50,51,85–87]. Histidine 189 is a proton acceptor for tyrosine D [50]. In contrast, our D•–D data on that same mutant show substantial alterations in ^{15}N sensitive regions of the spectrum, consistent with a contribution from this histidine to the spectrum [50,51]. Also, we have demonstrated that a different substitution at histidine 189, HL189D2, gives a spectrum similar to the YF160D2 mutant, in agreement with the results of EPR control experiments [24,37,50,51,85–87].

We observe a 1504 cm^{-1} line in our infrared spectra of D•–D, obtained by either flash or continuous illumination; this line does not show significant intensity differences or frequency shifts with $^{13}C(6)$, $^{13}C(1)$ or 3,5-$^{2}H(2)$ labeling of tyrosine. Therefore, we do not favor the assignment of this feature in our spectra to D•.

4.8. Possible explanations for the results leading to the alternative assignment of D•–D

It is our hypothesis that the alternative spectrum of Refs. [44,45] does not reflect a physiologically relevant oxidation spectrum of tyrosine D. In our view, possible reasons for this discrepancy are: (1) a low yield of D• in the samples employed in Refs. [44,45]; (2) aggregation of PSII under the conditions employed; (3) contributions to the difference spectrum from the protonation of phosphate and formate; and (4) use of kinetic transients in a time regime where oxidation/reduction of tyrosine D cannot be observed. In this previous work [44], only two kinetic

transients were used to construct a difference spectrum. It is possible to ratio two such transients and to construct a difference spectrum that has little or no contribution from D• and exhibits either small or negligible amplitude at 1477 cm^{-1} (see for example, Fig. 10C, D1/D2). The time interval in which such cancellation will occur depends on the total yield of D• and on the details of its decay kinetics. In Ref. [44], EPR control experiments were performed differently, when compared to FT-IR experiments. In the FT-IR experiments, flashes were given every 12 min, while in the EPR experiments, flashes were given every 3.3 min.

4.9. Other FT-IR results in the literature

In our reading of the literature, there is no previous report in contradiction with our conclusions. For example, in the elegant step scan experiments of Ref. [81], a change in decay rate in the presence and absence of DCMU was used to assign the 1478/1477 cm^{-1} line to Q_A^-. However, infrared data obtained in the presence and absence of DCMU were obtained with different repetition rates, which would be expected to change the magnitude of tyrosine D contributions to the spectrum, while leaving the tyrosine Z contributions unaltered. This may be the origin of the apparent alterations in the decay rate of the 1478 cm^{-1} line obtained in the presence and absence of DCMU.

In the experiments of Refs. [46,88–90] on manganese containing PSII membranes, an infrared spectrum, attributed to $S_2Q_A^-$–S_1Q_A, has vibrational features, assigned to Q_A^-–Q_A, which are similar to our D•–D spectrum. Long-term dark-adapted samples were employed in this work [46,90]. Such samples are predominantly in the S_1 state, and, in this case, a significant percentage of tyrosine D• is reduced in the dark. Illumination of such a sample at 250 K will have the effect of generating the S_2 state, which in turn will oxidize tyrosine D [31,32], giving an overall D•–D contribution to the vibrational spectrum. Therefore, a D•–D assignment of this difference FT-IR spectrum is actually a reasonable interpretation of the data presented [46,88–90]. By contrast, our EPR control experiments have shown that our $S_2Q_A^-$–S_1 Q_A spectrum (presented here) does not exhibit such a D•–D contribution or an intense 1478 cm^{-1} line [63,64]. In more recent work [46], this group has obtained a $S_2Q_A^-$–S_1 Q_A spectrum on *Synechocystis* PSII samp1es. When the spinach and *Synechocystis* $S_2Q_A^-$–S_1 Q_A spectra are compared, the intensity of a positive 1478 cm^{-1} mode is significantly increased in the *Synechocystis* spectrum. The increase in relative intensity of the 1478 cm^{-1} in cyanobacterial PSII is interesting and may correlate with an increased contribution from tyrosine D oxidation.

4.10. General conclusions

Based on assignments in the literature, the 1478/1477 cm^{-1} line could arise from tyrosyl radicals, from Q_A^-, from chlorophyll cation radicals, or from multiple species with overlapping contributions. Our experiments show conclusively, that in both spinach and cyanobacterial PSII at pH 7.5, a component of the 1478/1477 cm^{-1} line arises from the tyrosyl radicals. Under continuous illumination in cyanobacterial PSII, our data support the previous conclusion that there are overlapping contributions in this region [49]. We favor the deduction that the origin of the other, non-tyrosyl, spectral component is a chlorophyll cation radical in cyanobacterial PSII. This conclusion is based on the ^{15}N sensitivity observed for the residual 1478 cm^{-1} line, observed previously in the presence of hydroxylamine [49], and the inverse correlation shown herein between the intensity of spectral contributions in this region and Q_A^- content. In spinach PSII, our previous work [49] also provides evidence for multiple contributions at 1478/1477 cm^{-1}. In spinach, the origin of the other component(s) at 1478/1477 cm^{-1} is either a chlorophyll cation radical, Q_A^-, or both. We favor the chlorophyll cation radical assignment, but, as we have stated previously [49], plastoquinone labeling is required to identify the Q_A and Q_A^- contributions in both spinach and cyanobacterial samples.

Difference FT-IR spectroscopy has the potential to give new insight into the functional mechanism of PSII. Progress in this technique requires firm vibrational assignments. To obtain vibrational assignments of in vivo spectra, site-directed mutagenesis and selective isotopic labeling experiments are critical. In this work, we present a series of experiments, which support the assignment of the positive 1478/

1477 cm^{-1} bands to lines involving a ν(C–O) stretch and arising from the tyrosyl radicals in photosystem II. Also, we have clarified several points raised in the literature regarding this assignment. With explicit vibrational assignments, it will be possible to obtain detailed insight in the local conformational changes in the protein backbone, in redox-active amino acids, and in cofactors that accompany charge separation and stabilization.

Acknowledgements

We thank Dr. Albert Markhart III and his group for generous use of the fluorometer. We thank Dr. Qing Yan for her initial efforts on the infrared flash measurements, and A. Ouellette and Dr. L. Anderson for providing PSII membrane preparations.

References

[1] A. Angerhofer, R. Bittl, Photochem. Photobiol. 63 (1996) 11–38.
[2] R.D. Britt, in: D.R. Ort, C.F. Yocum, (Eds.), Oxygenic Photosynthesis: The Light Reactions, Vol. 4, Kluwer Academic Publisher, Dordrecht (1996), pp. 137–164.
[3] O. Nanba, K. Satoh, Proc. Natl. Acad. Sci. U.S.A. 84 (1987) 109–112.
[4] M.R. Wasielewski, D.G. Johnson, M. Seibert, Govindjee, Proc. Natl. Acad. Sci. U.S.A. 86 (1989) 524–528.
[5] G. Hastings, J.R. Durrant, J. Barber, G. Porter, D. Klug, Biochemistry 31 (1992) 7638–7647.
[6] M.B. Muller, M. Hucker, M. Reus, A.R. Holzwarth, J. Phys. Chem. 100 (1996) 9527–9536.
[7] B. Donovan, L.A. Walker, D. Kaplan, M. Bouvier, C.F. Yocum, R.J. Sension, J. Phys. Chem. 100 (1997) 1945–1949.
[8] A.M. Nuijs, H.J. van Gorkom, J.J. Plijter, L.N.M. Duysens, Biochim. Biophys. Acta 848 (1986) 167–175.
[9] G.H. Schatz, A.R. Holzwarth, in: J. Biggins (Ed.), Progress in Photosynthesis Research, Vol. 1, Martinus Nijhoff Publishers, the Hague, the Netherlands (1987) p. 67.
[10] H.-J. Eckert, N. Wiese, J. Bernarding, H.-J. Eichler, G. Renger, FEBS Lett. 240 (1988) 153–158.
[11] H.-W. Trissl, W. Leibl, FEBS Lett. 244 (1989) 85–88.
[12] A.R. Crofts, C.A. Wraight, Biochim. Biophys. Acta 726 (1983) 149–185.
[13] S. Gerken, K. Brettel, E. Schlodder, H.T. Witt, FEBS Lett. 237 (1988) 69–75.
[14] G.T. Babcock, R.E. Blankenship, K. Sauer, FEBS Lett. 61 (1976) 286–289.
[15] J.P. Dekker, J.J. Plijter, L. Ouwehand, H.J. van Gorkom, Biochim. Biophys. Acta 767 (1984) 176–179.
[16] M.R. Razeghifard, C. Klughammer, R.J. Pace, Biochemistry 36 (1997) 86–92.
[17] M. Boska, K. Sauer, W. Buttner, G.T. Babcock, Biochim. Biophys. Acta 722 (1983) 327–330.
[18] G.T. Babcock, K. Sauer, Biochim. Biophys. Acta 376 (1975) 329–344.
[19] G.T. Babcock, K. Sauer, Biochim. Biophys. Acta 376 (1975) 315–328.
[20] R.J. Boerner, B.A. Barry, J. Biol. Chem. 268 (1993) 17151–17154.
[21] R.J. Debus, B.A. Barry, I. Sithole, G.T. Babcock, L. McIntosh, Biochemistry 27 (1988) 9071–9074.
[22] J.G. Metz, P.J. Nixon, M. Rogner, G.W. Brudvig, B.A. Diner, Biochemistry 28 (1989) 6960–6969.
[23] G.H. Noren, B.A. Barry, Biochemistry 31 (1992) 3335–3342.
[24] D.A. Force, D.W. Randall, R.D. Britt, X.-S. Tang, B.A. Diner, J. Am. Chem. Soc. 117 (1995) 12643–12644.
[25] U. Sun, X.-S. Tang, B. Diner, Biochemistry 35 (1996) 679–684.
[26] X.S. Tang, M. Zheng, D.A. Chisholm, G.C. Dismukes, B.A. Diner, Biochemistry 35 (1996) 1475–1484.
[27] M.T. Bernard, G.M. MacDonald, A.P. Nguyen, R.J. Debus, B.A. Barry, J. Biol. Chem. 270 (1995) 1589–1594.
[28] B.A. Barry, G.T. Babcock, Proc. Natl. Acad. Sci. U.S.A. 84 (1987) 7099–7103.
[29] R.J. Debus, B.A. Barry, G.T. Babcock, L. McIntosh, Proc. Natl. Acad. Sci. U.S.A. 85 (1988) 427–430.
[30] W.F.J. Vermaas, A.W. Rutherford, O. Hansson, Proc. Natl. Acad. Sci. U.S.A. 85 (1988) 8477–8481.
[31] G.T. Babcock, K. Sauer, Biochim. Biophys. Acta 325 (1973) 483–503.
[32] G.T. Babcock, K. Sauer, Biochim. Biophys. Acta 325 (1973) 504–519.
[33] C.A. Buser, L.K. Thompson, B.A. Diner, G.W. Brudvig, Biochemistry 29 (1990) 8977–8985.
[34] R.J. Boerner, K.A. Bixby, A.P. Nguyen, G.H. Noren, R.J. Debus, B.A. Barry, J. Biol. Chem. 268 (1993) 1817–1823.
[35] R.G. Evelo, S.A. Dikanov, A.J. Hoff, Chem. Phys. Lett. 157 (1989) 25–30.
[36] I.D. Rodriguez, T.K. Chandrashekar, G.T. Babcock, in: J. Biggins (Ed.), Progress in Photosynthesis Research, Vol. I, Martinus Nijhoff Publishers, Dordrecht (1987) pp. 471-473.
[37] X.-S. Tang, D.A. Chisholm, G.C. Dismukes, G.W. Brudvig, B.A. Diner, Biochemistry 32 (1993) 13742–13748.
[38] M. Engelhard, K. Gerwert, B. Hess, W. Kreutz, F. Seibert, Biochemistry 24 (1985) 400–407.
[39] G. Dollinger, L. Eisenstein, S.-L. Lin, K. Nakanishi, J. Termini, Biochemistry 25 (1986) 6524–6533.
[40] K.J. Rothschild, P. Roepe, P.L. Ahl, T.N. Earnest, R.A. Bogomolni, S.K.D. Gupta, C.M. Mulliken, J. Herzfeld, Proc. Natl. Acad. Sci. U.S.A. 83 (1986) 347–351.
[41] A.J. Hoff, J. Deisenhofer, Phys. Rep. 287 (1997) 1–247.
[42] C. Berthomieu, E. Nabedryk, W. Mantele, J. Breton, FEBS Lett. 269 (1990) 363–367.

[43] C. Berthomieu, E. Nabedryk, J. Breton, A. Boussac, in: N. Murata (Ed.), Research in Photosynthesis, Vol. II, Kluwer, Dordrecht, the Netherlands (1992) pp. 53-56.
[44] R. Hienerwadel, A. Boussac, J. Breton, C. Berthomieu, Biochemistry 35 (1996) 15447–15460.
[45] R. Hienerwadel, A. Boussac, J. Breton, B.A. Diner, C. Berthomieu, Biochemistry 36 (1997) 14712–14723.
[46] T. Noguchi, Y. Inoue, X.-S. Tang, Biochemistry 36 (1997) 14705–14711.
[47] G.M. MacDonald, B.A. Barry, Biochemistry 31 (1992) 9848–9856.
[48] G.M. MacDonald, K.A. Bixby, B.A. Barry, Proc. Natl. Acad. Sci. U.S.A. 90 (1993) 11024–11028.
[49] G.M. MacDonald, J.J. Steenhuis, B.A. Barry, J. Biol. Chem. 270 (1995) 8420–8428.
[50] S. Kim, J. Liang, B.A. Barry, Proc. Natl. Acad. Sci. U.S.A. 94 (1997) 14406–14411.
[51] S. Kim, B.A. Barry, Biophys. J. 74 (1998) 2588–2600.
[52] J.S. Patzlaff, B.A. Barry, Biochemistry 35 (1996) 7802–7811.
[53] D.A. Berthold, G.T. Babcock, C.F. Yocum, FEBS Lett. 134 (1981) 231–234.
[54] D.F. Ghanotakis, D.M. Demetriou, C.F. Yocum, Biochim. Biophys. Acta 891 (1987) 15–21.
[55] J.G.K. Williams, Methods Enyzmol. 167 (1988) 766–778.
[56] R. Rippka, J. Derulles, J.B. Waterbury, M. Herdman, R. Stanier, J. Gen. Microbiol. 111 (1979) 1–61.
[57] G.H. Noren, R.J. Boerner, B.A. Barry, Biochemistry 30 (1991) 3943–3950.
[58] B.A. Barry, Methods Enzymol. 258 (1995) 303–319.
[59] C.F. Yocum, C.T. Yerkes, R.E. Blankenship, R.R. Sharp, G.T. Babcock, Proc. Natl. Acad. Sci. U.S.A. 78 (1981) 7507–7511.
[60] W.E. Peiffer, R.T. Ingle, S. Ferguson-Miller, Biochemistry 29 (1990) 8696–8701.
[61] H.K. Lichtenthaler, Methods Enzymol. 148 (1987) 350–382.
[62] G.T. Babcock, D.F. Ghanotakis, B. Ke, B.A. Diner, Biochim. Biophys. Acta 723 (1983) 276–286.
[63] J.J. Steenhuis, B.A. Barry, J. Am. Chem. Soc. 118 (1996) 11927–11932.
[64] J.J. Steenhuis, B.A. Barry, J. Phys. Chem. B 101 (1997) 6652–6660.
[65] I. Vass, S. Styring, Biochemistry 30 (1991) 830–839.
[66] A.-F. Miller, G.W. Brudvig, Biochim. Biophys. Acta 1056 (1991) 1–18.
[67] P. Joliot, A. Joliot, Biochim. Biophys. Acta 305 (1973) 302–316.
[68] V. Petrouleas, B.A. Diner, Biochim. Biophys. Acta 849 (1986) 264–275.
[69] V.V. Klimov, E. Dolan, E.R. Shaw, B. Ke, Proc. Natl. Acad. Sci. U.S.A. 77 (1980) 7227–7231.
[70] R.J. Boerner, A.P. Nguyen, B.A. Barry, R.J. Debus, Biochemistry 31 (1992) 6660–6672.
[71] L.H. Jones, Inorg. Chem. 2 (1963) 777–780.
[72] B. Barry, R.A. Mathies, Biochemistry 26 (1987) 59–64.
[73] D.F. Ghanotakis, G.T. Babcock, FEBS Lett. 153 (1983) 231–234.
[74] C.W. Hoganson, G.T. Babcock, Biochemistry 28 (1989) 1448–1454.
[75] R.J. Debus, Biochim. Biophys. Acta 1102 (1992) 269–352.
[76] R. Hienerwadel, D. Thibodeau, F. Lenz, E. Nabedryk, J. Breton, W. Kreutz, W. Mantele, Biochemistry 31 (1992) 5799–5808.
[77] R. Hienerwadel, C. Berthomieu, Biochemistry 34 (1995) 16288–16297.
[78] Y. Qin, R.A. Wheeler, J. Am. Chem. Soc. 117 (1995) 6083–6092.
[79] C. Ma, B.A. Barry, Biophys. J. 71 (1996) 1961–1972.
[80] G.N.R. Tripathi, R.H. Schuler, J. Chem. Phys. 81 (1984) 113–121.
[81] H. Zhang, M.R. Razeghifard, G. Fischer, T. Wydryzinski, Biochemistry 36 (1997) 11762–11768.
[82] G.N.R. Tripathi, R.H. Schuler, J. Phys. Chem. 91 (1987) 5881–5885.
[83] Y. Qin, R.A. Wheeler, J. Chem. Phys. 102 (1995) 1689–1698.
[84] J.B. Ames, M. Ros, J. Raap, J. Lugtenburg, R.A. Mathies, Biochemistry 31 (1992) 5328–5334.
[85] C. Tommos, L. Davidsson, B. Svennson, C. Madsen, W. Vermaas, S. Styring, Biochemistry 32 (1993) 5436–5441.
[86] S. Un, X.-S. Tang, B.A. Diner, Biochemistry 35 (1996) 679–684.
[87] K.A. Campbell, J.M. Peloquin, B.A. Diner, X.-S. Tang, D.A. Chisholm, R.D. Britt, J. Am. Chem. Soc. 119 (1997) 4787–4788.
[88] T. Noguchi, T.-A. Ono, Y. Inoue, Biochemistry 31 (1992) 5953–5956.
[89] T. Noguchi, T.-A. Ono, Y. Inoue, Biochim. Biophys. Acta 1143 (1993) 333–336.
[90] T. Noguchi, T.-A. Ono, Y. Inoue, Biochim. Biophys. Acta 1232 (1995) 59–66.